

國立臺灣大學電機資訊學院電信工程學研究所

碩士論文

Graduate Institute of Communication Engineering  
College of Electrical Engineering & Computer Science

National Taiwan University

Master Thesis

可適性水聲通道追蹤之最佳遺忘因子估測

Forgetting Factor Estimation for Adaptive  
UWA Channel Tracking



Hsu Che-Wei

指導教授：曹建和 博士

Advisor: Tsao Jenho, Ph.D.

中華民國 98 年 6 月

June, 2009

# 國立臺灣大學碩士學位論文 口試委員會審定書

可適性水聲通道追蹤之最佳遺忘因子估測

Forgetting Factor Estimation for Adaptive UWA Channel Tracking

本論文係許哲瑋君 (R96942123) 在國立臺灣大學電信工程學研究所完成之碩士學位論文，於民國 98 年 6 月 27 日承下列考試委員審查通過及口試及格，特此證明

口試委員：



\_\_\_\_\_ (指導教授)

\_\_\_\_\_  
\_\_\_\_\_  
\_\_\_\_\_

系主任、所長

\_\_\_\_\_ (簽名)

# Acknowledgements

First of all I would like to thank my family who has sacrificed so much of all that was theirs to give me a good education. I cannot even begin to thank them for all they have done for me.

My sincerest thanks to my thesis supervisor, Dr. Tsao, for his encouragement and guidance throughout this thesis research and my graduate study in the NTU-GICE.

And I would like to thank all my lab-mates for their great company on those long days spent at NTU. I have profited considerably from discussions with several friends and colleagues on several problems, although not necessarily related to this thesis. Special thanks to David Huang for some supports of signal processing techniques. Finally I would like to thank PeePee. I would be nowhere without her constant love and support throughout my time here, this thesis would not be possible without her.



# 中文摘要

水聲通訊和無線電通訊主要有二個最大的差異點，一是水聲通道有非常長的多重路徑延遲，範圍可涵蓋十到一百多個符號(symbols)，另一個是通道時變的速度。對於基於通道估測的等化器來說，通道估測是決定其效能的表現的最重要因素。在本篇論文中以遞迴性最小平方方法做於通道追蹤的演算法，在這種演算法中若使用固定的遺忘因子去追蹤時變通道是不適合的，因為若當遺忘因子接近1時收斂會變慢，但當遺忘因子過小時又有錯誤調整過大的問題。所以水聲環境的通道追蹤必需可適性的調整遺傳因子以得到較好的追蹤效能，論文中我們提出一種較為直接的方法，以一種實現理論最佳值的方法來設定遺傳因子，取代以往以殘差均方誤差做於依據來調整遺傳因子的方法。最後實驗的效能表現是以「ASIAEX」的資料做為測試來源，在實驗中會以「信號多徑比」(SMR)做為衡量通道狀況的好壞。在實驗結果中，可以觀察到我們提出的遺傳因子估測法非常的有效，即時在較為嚴重的衰落通道也能預測準確，且可以發現的是最佳因子的值和通道的時變速度、「信號多徑比」有很大的關聯。

關鍵字:遺忘因子、通道追蹤、通道估測、水聲通道、遞迴性最小平方方法

# Abstract

Underwater acoustic communications differ from RF communications in two major aspects. One is the long multipath delay time covering tens to hundreds of symbols and the other is temporal variation of the acoustic channel at a time scale on the order of communication packet length. And the precision of channel estimation is the critical factor for the performance of channel estimation based equalizer. Here we using recursive least square algorithm as channel tracking algorithm. The RLS algorithm with a constant forgetting factor (FF) is not suitable for tracking time-varying channel because its convergence is slow when the FF is close to one, whereas the misadjustment is large when the FF is small. Therefore, the forgetting factor of RLS algorithm needs to be set adaptively in order to yield satisfactory performance in UWA environments. In this thesis, we provide a more directly method, say, from implementation of theoretical optimal value to set the FF, instead of controlling the forgetting factor based on the residual mean square error. The experiment result was presented based on ASIAEX data, and SMR was used as a measure for charactering the general quality of the channel. In the experiment result, we can observe that the proposed Forgetting Factor estimation is effective, even for severe fading channel. And it's obvious that the value of optimal Forgetting Factor is highly correlated to the channel fading rate and SMR.

Key word: forgetting factor 、 channel tracking 、 channel estimation 、 underwater acoustic channel 、 Recursive Least Square algorithm

## Table Of Contents:

口試委員會審定書.....	i
誌謝.....	ii
中文摘要.....	iii
英文摘要.....	iv
Chapter 1 Introduction .....	1
1.1 A brief background of underwater acoustic communications.....	1
1.2 The Ocean Acoustic Environment.....	5
1.2.1 Ambient noise.....	8
1.2.2 Internal waves.....	9
1.3 An introduction to Channel Estimation.....	10
1.3.1 Why Channel Estimation? .....	10
1.3.2 Training Sequences and Blind Method.....	12
1.4 Forgetting factor estimation overview.....	14
1.5 Research motivation.....	15
1.6 Thesis overview.....	16
Chapter 2 Underwater acoustic channel estimation and channel tracking .....	17
2.1 Channel estimation by pulse compression.....	17
2.2 Channel tracking by Recursive Least Squares (RLS) algorithm.....	19
2.3 The impact of channel estimation error on the equalizer.....	25
2.4 AR channel model.....	28
2.5 The optimal forgetting factor of RLS for channel estimation.....	31
Chapter 3 Optimal forgetting factor estimation.....	33

3.1 Implementation of forgetting factor estimation.....	33
3.2 Doppler-Spread estimation.....	38
3.3 Compute the approximate optimal forgetting factor.....	45
Chapter 4 Experiment Result.....	48
4.1 The Asian Seas International Acoustics Experiment (ASIAEX).....	48
4.2 Signal-To-Multipath Ratio (SMR).....	53
4.3 Performance & Results.....	59
Chapter 5 Conclusion.....	73
Reference.....	74



## Table of Figures:

Fig. 2-1 Shift register for the creation of the m-sequence signal.....	18
Fig. 2-2 Adaptive filter.....	20
Fig. 2-3 system model.....	26
Fig. 2-4 CE-DFE.....	27
Fig. 2-5 linear equalizer.....	27
Fig. 2-6 AR model.....	30
Fig. 3-1 optimal forgetting factor for ASIAEX data-day 126-6:15:32.....	34
Fig. 3-2 transmission data format.....	36
Fig. 3-3 window shift one bit.....	36
Fig. 3-4 channel impulse response in time domain and delay domain.....	41
Fig. 3-5 The scattering function.....	42
Fig. 3-6 The direct-path spectrum.....	43
Fig. 3-7 The scattering function and the direct path spectrum.....	45
Fig. 3-8 transmission format.....	47
Fig.4-1 Geometry of the transmission experiment.....	49
Fig.4-2 channel condition-ASIAEX day126-6:17:58.....	50
Fig.4-3 channel condition-ASIAEX day 128-9:46:2.....	51
Fig.4-4 channel condition-ASIAEX day 128- 12:50:04.....	53
Fig. 4-5 channel impulse response and the ISI.....	55
Fig. 4-6 SMR of different channels.....	56
Fig. 4-7 channel 15, 13, 8, 2 impulse response by pulse compression.....	56
Fig. 4-8 SMR for different receiving time.....	57
Fig. 4-9 Instantaneous channel impulse response by pulse compression.....	58
Fig. 4-10 SMR of channel 1~16 (day 126 - 6:15:17).....	60



Fig. 4-11 CIR of channel 1~16 (day 126 - 6:15:17).....	60
Fig. 4-12 scattering function of channel 1~16 (day 126 - 6:15:17).....	61
Fig. 4-13 performance of optimal forgetting factor prediction(M=10).....	62
Fig. 4-14 performance of optimal forgetting factor prediction (M=20).....	63
Fig. 4-15 performance of optimal forgetting factor prediction(M=30).....	64
Fig. 4-16 channel estimation error (day 126 - 6:15:17).....	64
Fig. 4-17 SMR of channel 1~16 (day 128-9:46:53).....	65
Fig. 4-18 CIR of channel 1~16 (day 128-9:46:53).....	65
Fig. 4-19 scattering function of channel 1~16 (day 128-9:46:53).....	66
Fig. 4-20 performance of optimal forgetting factor prediction (M=20).....	67
Fig. 4-21 channel estimation error (day 128-9:46:53).....	67
Fig. 4-22 SMR of channel 1~16 (day 128-12:46:03).....	68
Fig. 4-23 CIR of channel 1~16 (day 128-12:46:03).....	68
Fig. 4-24 scattering function of channel 1~16 (day 128-12:46:03).....	69
Fig. 4-25 performance of optimal forgetting factor prediction (M=20).....	69
Fig. 4-26 channel estimation error (day 128-12:46:03).....	70
Fig.4-27 optimal forgetting factor comparison of these three cases.....	71
Fig.4-28 minimum channel estimation MSE comparison of these three cases.....	72

# Chapter 1 Introduction

The past three decades have seen a growing interest in underwater acoustic communications because of its applications in marine research, oceanography, marine commercial operations, the offshore oil industry and defense. Continued research over the years has resulted in improved performance and robustness as compared to the initial communication systems.

## 1.1 A brief background of underwater acoustic communications

Underwater acoustic communication is a technique of sending and receiving message below water. There are several ways of doing such communication but the most common is using hydrophones. In underwater communication there are low data rates compared to terrestrial communication, since underwater communication uses acoustic waves instead of electromagnetic waves.

High-speed communication in the underwater acoustic channel has been challenging because of limited bandwidth, extended multipath, refractive properties of the medium, severe fading, rapid time variation and large Doppler shifts. In the initial years, rapid progress was made in deep water communication, but the shallow water channel was considered difficult. In the past decade, significant advances have been made in shallow water communication [1].

The shallow water acoustic communication channel exhibits a long delay spread because of numerous multipath arrivals resulting from surface and bottom interactions. Movement of transducers, ocean surface, and internal waves lead to rapid time variation and, consequently, a high Doppler spread in the channel. Coherent modulation schemes such as phase shift keying (PSK) along with adaptive decision feedback equalizers (DFE) and spatial diversity combining have been shown to be an effective way of communication in such channels. However, the long delay spread (often hundreds of symbols) and rapid time variation of the channel often makes this approach computationally too complex for real-time implementations.

Although the underwater channel has a long impulse response, the multipath arrivals are often discrete. This opens up the possibility of using a sparse equalizer with tap placement based on the actual channel response. This can potentially dramatically reduce the number of required taps and hence lead to a lower complexity, faster channel tracking and an enhanced performance.

Due to the symmetry of the linear wave equation, if the sound transmitted from one location is received at other locations, reversed and retransmitted, it focuses back at the original source location. This is the principle behind time reversal mirrors (TRM) or its frequency domain equivalent—active phase conjugation. The temporal compression effect of TRM reduces the delay spread of the channel while the spatial focusing effect

improves signal-to-noise ratio (SNR) and reduces fading. In fact, the spatial focusing precludes the use of multiple receivers for spatial diversity, but opens up the possibility of spatial multiplexing and low probability of intercept (LPI) communications.

Although TRM helps reduce delay spread of the channel, it does not eliminate ISI completely. By implementing a DFE at a TRM receiver, the communication performance can be further improved. In a TRM-based communication system, a probe signal has to be first transmitted from the receiver to the transmitter. The transmitter then uses a time-reversed version of this signal to convey information. As the channel changes over time, the probe signal has to be retransmitted to sample the channel but decoherence times up to several tens of minutes were observed at frequencies of 3.5 kHz during experiments. A closely related idea—passive phase conjugation (PPC)—uses the cross-correlation of two consecutive signals transmitted from the transmitter to the receiver to convey information.

Progress in underwater acoustic telemetry since 1982 is reviewed within a framework of six current research areas: 1) underwater channel physics, channel simulations, and measurements; 2) receiver structures; 3) diversity exploitation; 4) error control coding; 5) networked systems; and 6) alternative modulation strategies[2].

1) The purpose of channel simulations is commonly to aid in evaluation of signal processing algorithms in an attempt to increase the success of field experiments. Less

common are attempts to use these models to explicitly relate time-varying ocean processes to telemetry performance and gain true insight. While there are numerous modeling techniques for underwater acoustic wave propagation including modal decompositions, parabolic equation methods, wave-number integration algorithms, and finite difference solutions, the telemetry community has focused almost exclusively, and appropriately, on ray theory.

2) While the substantial attenuation of underwater communication signals as well as pervasive noise sources (anthropogenic, biological, and wave phenomena) often conspire to reduce available SNR, the phenomenon of reverberation, in both time and frequency, has tended to dominate the evolution of receiver strategies for underwater acoustic telemetry. Incoherent receivers have generally sought to avoid reverberation issues using classical methods while coherent receivers have struggled to accommodate reverberation with new powerful adaptive algorithms.

3) Classical diversity in a communication system refers to the availability of multiple, uncorrelated measurements of the transmitted signal. These measurements may be taken over different frequency bands, temporal spans, or spatial apertures. Such diversity is a powerful tool in combating the effects of fading channels characterized by a complex amplitude scaling that is a random variable leading to periods of low SNR.

4) Coding of communication signals classically falls into one of two categories:

source coding in which redundancy is removed from the information to be transmitted and channel coding in which structured redundancy is added to the signal to provide protection against errors. Both have found widespread application in underwater acoustic telemetry.

5) The last five years have witnessed a surge of interest in underwater acoustic networks. Although sporadic interest in multiple point communication is found in earlier literature, the relatively recent emphasis on synoptic, spatially sampled oceanographic surveillance has provided an impetus to the transfer of networked communication technology to the underwater environment.

6)FSK and QAM, in their various forms, have dominated digital underwater acoustic communication applications. Some researchers, however, have begun to explore alternative modulation schemes motivated largely by the need to mitigate temporal reverberation of the channel.

## **1.2 The Ocean Acoustic Environment**

Underwater acoustic propagation depends on many factors. The direction of sound propagation is determined by the sound speed gradients in the water. In the sea the vertical gradients are generally much larger than the horizontal ones. These facts, combined with a tendency for increasing sound speed with increasing depth due to the

increasing pressure in the deep sea reverses the sound speed gradient in the thermocline creating an efficient waveguide at the depth corresponding to the minimum sound speed.

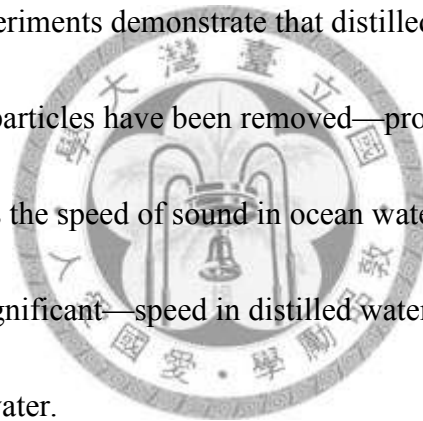
The sound speed profile may cause regions of low sound intensity called "Shadow Zones" and regions of high intensity called "Caustics". These may be found by ray tracing methods.

At equatorial and temperate latitudes in the ocean the surface temperature is high enough to reverse the pressure effect, such that a sound speed minimum occurs at depth of a few hundred meters. The presence of this minimum creates a special channel known as Deep Sound Channel, previously known as the SOFAR (sound fixing and ranging) channel, permitting guided propagation of underwater sound for thousands of kilometres without interaction with the sea surface or the seabed. Another phenomenon in the deep sea is the formation of sound focusing areas known as Convergence Zones. In this case sound is refracted downward from a near-surface source and then back up again. The horizontal distance from the source at which this occurs depends on the positive and negative sound speed gradients. A surface duct can also occur in both deep and moderately shallow water when there is upward refraction, for example due to cold surface temperatures. Propagation is by repeated sound bounces off the surface.

The speed of sound depends on the medium through which sound waves propagate. The speed of sound differs in air and water, with sound waves traveling faster in water.

For example, in air at a temperature of 18°C (64°F), the speed of sound is approximately 341 meters (1,120 feet) per second. In contrast, in salt water at approximately the same temperature, the speed of sound is approximately 1,524 meters (5,000 feet) per second.

The state properties of water (temperature and pressure) and the degree of salinity also affect the speed of sound. The propagation of sound waves in sea water can be directly affected by suspensions of particulate matter that can scatter, absorb, or reflect the waves. Laboratory experiments demonstrate that distilled water—water from which salts and other suspended particles have been removed—provides a medium in which the speed of sound exceeds the speed of sound in ocean water. The difference in the speed of transmission is significant—speed in distilled water may be 20 to 30 times that of speeds found in ocean water.



Because frequency and wavelength are inversely proportional characteristics of sound waves, low-frequency signals produce long sound wavelengths. These long-wavelength signals encounter fewer suspended particles as they pass through the medium and thus are not as subject to scattering, absorption, or reflection. As a result, low-frequency signals are able to travel farther without significant loss of signal strength.



### 1.2.1 Ambient noise

Measurement of acoustic signals are possible if their amplitude exceeds a minimum threshold, determined partly by the signal processing used and partly by the level of background noise. Ambient noise is that part of the received noise that is independent of the source, receiver and platform characteristics. This it excludes reverberation and towing noise for example.

The background noise present in the ocean, or ambient noise, has many different sources and varies with location and frequency.[3] At the lowest frequencies, from about 0.1 Hz to 10 Hz, ocean turbulence and microseisms are the primary contributors to the noise background. Typical noise spectrum levels decrease with increasing frequency from about 140 dB re  $1 \mu\text{Pa}^2/\text{Hz}$  at 1 Hz to about 30 dB re  $1 \mu\text{Pa}^2/\text{Hz}$  at 100 kHz. Distant ship traffic is one of the dominant noise sources in most areas for frequencies of around 100 Hz, while wind-induced surface noise is the main source between 1 kHz and 30 kHz. At very high frequencies, above 100 kHz, thermal noise of water molecules begins to dominate. The thermal noise spectral level at 100 kHz is 25 dB re  $1 \mu\text{Pa}^2/\text{Hz}$ . The spectral density of thermal noise increases by 20 dB per decade (approximately 6 dB per octave).

Transient sound sources also contribute to ambient noise. These can include intermittent geological activity, such as earthquakes and underwater volcanoes, rainfall

on the surface, and biological activity. Biological sources include cetaceans (especially blue, fin and sperm whales), certain types of fish, and snapping shrimp.

### **1.2.2 Internal waves**

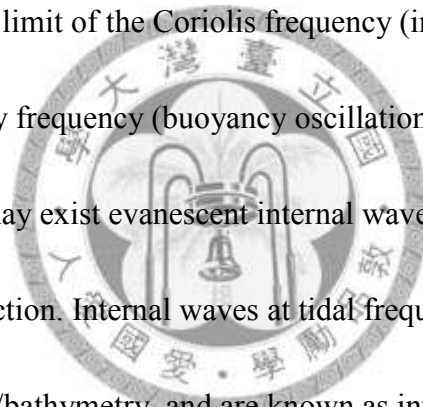
Internal waves are gravity waves that oscillate within, rather than on the surface of, a fluid medium. They arise from perturbations to hydrostatic equilibrium, where balance is maintained between the force of gravity and the buoyant restoring force. A simple example is a wave propagating on the interface between two fluids of different densities, such as oil and water. Internal waves typically have much lower frequencies and higher amplitudes than surface gravity waves because the density differences (and therefore the restoring forces) within a fluid are usually much smaller than the density of the fluid itself. Internal wave motions are ubiquitous in both the ocean and atmosphere.

Nonlinear solitary internal waves are called solitons.

The atmosphere and ocean are continuously stratified: potential density generally increases steadily downward. Internal waves in a continuously stratified medium may propagate vertically as well as horizontally. The dispersion relation for such waves is curious: For a freely-propagating internal wave packet, the direction of propagation of energy (group velocity) is perpendicular to the direction of propagation of wave crests and troughs (phase velocity). An internal wave may also become confined to a finite

region of altitude or depth, as a result of varying stratification or wind. Here, the wave is said to be ducted or trapped, and a vertically standing wave may form, where the vertical component of group velocity approaches zero. A ducted internal wave mode may propagate horizontally, with parallel group and phase velocity vectors, analogous to propagation within a waveguide.

At large scales, internal waves are influenced both by the rotation of the Earth as well as by the stratification of the medium. The frequencies of these geophysical wave motions vary from a lower limit of the Coriolis frequency (inertial motions) up to the Brunt-Väisälä, or buoyancy frequency (buoyancy oscillations). Above the Brunt-Väisälä frequency may exist evanescent internal wave motions, for example those resulting from partial reflection. Internal waves at tidal frequencies are produced by tidal flow over topography/bathymetry, and are known as internal tides. Similarly, Atmospheric tides arise from, for example, non-uniform solar heating associated with diurnal motion.



## **1.3 An introduction to Channel Estimation**

### **1.3.1 Why Channel Estimation?**

Before we approach the problem of predicting and analyzing the observable properties of transmission, we must first define what we mean by a channel. In its most

general sense, a channel can describe everything from the source to the sink of a radio (or acoustic) signal. This includes the physical medium (free space, fiber, waveguides etc.) between the transmitter and the receiver through which the signal propagates. The word channel refers to this physical medium throughout this work. An essential feature of any physical medium is, that the transmitted signal is received at the receiver, corrupted in a variety of ways by frequency and phase-distortion, inter symbol interference and thermal noise.

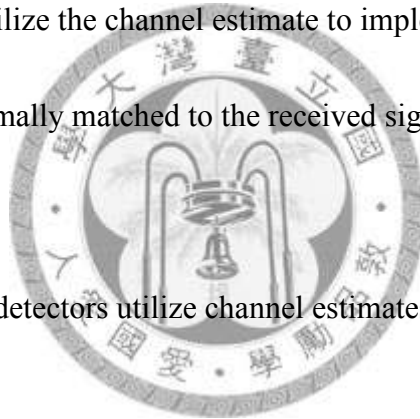
A channel model on the other hand can be thought of as a mathematical representation of the transfer characteristics of this physical medium. This model could be based on some known underlying physical phenomenon or it could be formed by fitting the best mathematical statistical model on the observed channel behavior. Most channel models are formulated by observing the characteristics of the received signals for each specific environment. Different mathematical models that explain the received signal are then fit over the accumulated data. Usually the one that best explains the behavior of the received signal is used to model the given physical channel.

Channel estimation is simply defined as the process of characterizing the effect of the physical channel on the input sequence. If the channel is assumed to be linear, the channel estimate is simply the estimate of the impulse response of the system. It must be stressed once more that channel estimation is only a mathematical representation of

what is truly happening. A “good” channel estimate is one where some sort of error minimization criteria is satisfied (e.g. MMSE).

Channel estimation algorithms allow the receiver to approximate the impulse response of the channel and explain the behavior of the channel. This knowledge of the channel's behavior is well-utilized in modern radio communications.

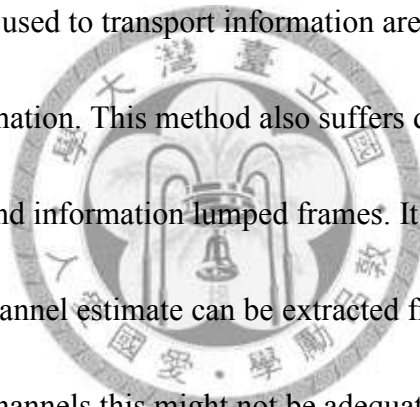
1. Adaptive channel equalizers utilize channel estimates to overcome the effects of inter symbol interference.
2. Diversity techniques utilize the channel estimate to implement a matched filter such that the receiver is optimally matched to the received signal instead of the transmitted one.
3. Maximum likelihood detectors utilize channel estimates to minimize the error probability.
4. One of the most important benefits of channel estimation is that it allows the implementation of coherent demodulation. Coherent demodulation requires the knowledge the phase of the signal. This can be accomplished by using channel estimation techniques.



### **1.3.2 Training Sequences and Blind Method**

Once a model has been established, its parameters need to be continuously updated

(estimated) in order to minimize the error as the channel changes. If the receiver has a-priori knowledge of the information being sent over the channel, it can utilize this knowledge to obtain an accurate estimate of the impulse response of the channel. This method is simply called Training sequence based Channel estimation. It has the advantage of being used in any radio communications system quite easily. Even though this is the most popular method in use today, it still has its drawbacks. One of the obvious drawbacks is that it is wasteful of bandwidth. Precious bits in a frame that might have been otherwise used to transport information are stuffed with training sequences for channel estimation. This method also suffers due to the fact that most communication systems send information lumped frames. It is only after the receipt of the whole frame that the channel estimate can be extracted from the embedded training sequence. For fast fading channels this might not be adequate since the coherence time of the channel might be shorter than the frame time.



Blind methods on the other hand require no training sequences. They utilize certain underlying mathematical information about the kind of data being transmitted. These methods might be bandwidth efficient but still have their own drawbacks. They are notoriously slow to converge (more than 1000 symbols may be required for an FIR channel with 10 coefficients). Their other drawback is that these methods are extremely computationally intensive and hence are impractical to implement in real-time systems.

They also do not have the portability of training sequence-based methods. One algorithm that works for a particular system may not work with another due to the fact they send different types of information over the channel.

## 1.4 Forgetting Factor Estimation Overview

Recursive least squares (RLS) algorithm has been used extensively in adaptive filtering, self-tuning control, system identification, prediction, and interference cancellation [4]. It is well known for its good convergence property and small

Mean square error (MSE) in stationary environments. However, the RLS algorithm with a constant forgetting factor (FF) is not suitable for tracking time-varying parameters because its convergence is slow when the FF is close to one, whereas the misadjustment is large when the FF is small. Therefore, the forgetting factor of RLS algorithm needs to be set adaptively in order to yield satisfactory performance in time-varying environments. Much effort has been directed to modifying the RLS algorithm. One modification uses a data weighting window on the input data sequence [5] to adjust the effective memory of the algorithm. However, it is not easy to adjust the window to the change. Another approach is to vary the forgetting factor according to the squared error [6]–[8]. This approach can maintain the standard RLS algorithm with the FF adjusted according to the error. The drawback of these methods is that the control of

FF is sensitive to measurement noise. Nevertheless, methods of this kind are widely employed in variable forgetting factor (VFF) RLS algorithms. Another approach is variable forgetting factor RLS adaptive algorithm, namely, the gradient-based VFF RLS algorithm (GVFF-RLS) [9]. The control of the forgetting factor is based on the gradient of the MSE rather than on the gradient of the instantaneous squared error. The success of the algorithm relies heavily on an improved mean square error analysis.

## 1.5 Research Motivation

In the following sections, we will state that the precision of channel estimation is the critical factor for the channel estimation based equalizer. Channel impulse response is not available and must be estimated and then tracked. Here we using recursive least square algorithm as channel tracking algorithm, and the forgetting value is the critical parameter of RLS. We can find that UWA channel is various and variable by using some metrics such as signal to multipath ration (SMR), Doppler spread, coherence time, etc. Those metrics are able to reflect the channel condition. So, adaptive adjustment of forgetting factor of RLS according to the channel condition to improve the accuracy of channel estimation is necessary. Even the receiving time is the same. It still can't explicitly confirm that all the receivers with different depth use the same forgetting factor to estimate each channel impulse response can all achieve minimum estimation



error. Underwater acoustic channel especially, which is confront various ambient noise, internal-wave, and unexpected situation. So our goal is to find and set the forgetting factor adaptively. This is the main issue we will discuss and present in this thesis.

## 1.6 Thesis Overview

This thesis is organized into five sections. We begin in Section II provides a thorough theoretical foundation for the concepts to follow, channel estimation, channel tracking, and the key element of equalizer performance. A first order AR process was used to model a time varying acoustic channel. Furthermore, degree of nonstationarity was introduced to provide a measure of the fluctuation rate of the channel under tracking. In Section III, we will discuss the proposed forgetting factor estimation and the implementation method. In Section IV, the experiment result was presented based on ASIAEX data, and SMR was used as channel characteristic metrics to reflect the channel fading

## **Chapter 2 Underwater acoustic channel estimation and channel tracking**

The UWA channels in acoustic communication systems are usually multipath fading channels, which are causing inter-symbol interference (ISI) in the received signal. To remove ISI from the signal, much kind of equalizers can be used. These equalizers require knowledge on the channel impulse response (CIR), which can be provided by a separate channel estimator. Usually the channel estimation is based on the known sequence of bits, which is unique for a certain transmitter and which is repeated in every transmission burst. Thus, the channel estimator is able to estimate CIR for each burst separately by exploiting the known transmitted bits and the corresponding received samples. In data transmission, CIR can be tracked adaptively by the channel tracking algorithms.

### **2.1 Channel estimation by Pulse Compression**

In this section, we will describe the use of the m-sequence (Maximum Length Sequence) signal for the measurement of channel impulse responses, in alternative to the traditional techniques based on the use of impulsive sources.

The m-sequence signal is well known since at least two decades: it is a binary sequence, in which each value can be simply 0 or 1, obtained by a shift register as the

one shown in Fig.2-1

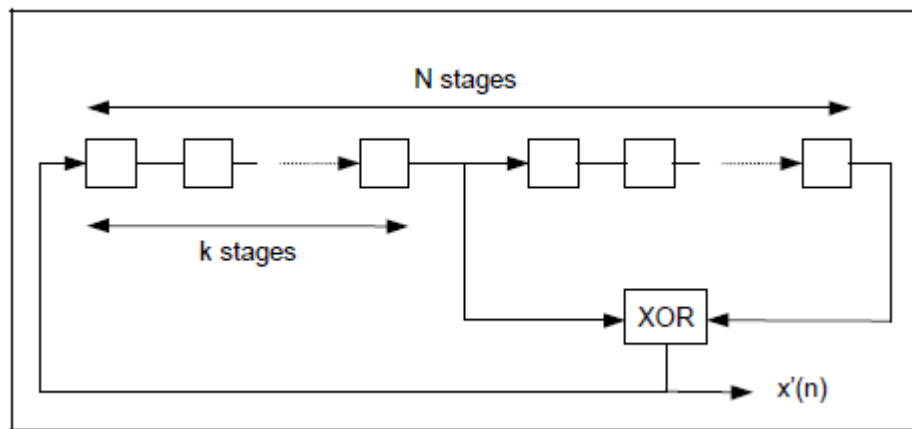


Figure 2-1 Shift register for the creation of the m-sequence signal

The obtained signal is periodic, with period of length  $L$  given by:

$$L=2^N-1$$

in which  $N$  is the number of slots in the shift register, also called the order of the m-sequence. Thus an order  $N=16$  means a sequence with a period of 65535 samples.

If a linear time invariant (LTI) system's impulse response is to be measured using a m-sequence, the response can be extracted from the measured system output  $y[n]$  by taking its circular cross-correlation with the m-sequence sequence. This is because the autocorrelation of an m-sequence is 1 for zero-lag, and nearly zero ( $-1/N$  where  $N$  is the sequence length) for all other lags; in other words, the autocorrelation of the m-sequence can be said to approach unit impulse function as m-sequence length increases. So we can use this property to obtain the channel impulse response [10].

If the channel impulse response is  $h[n]$ , the transmitted m-sequence is  $d[n]$ , the received signal is  $y[n]$ , then

$$y[n] = h[n] * d[n]$$

where,  $*$  denote convolution operation.

Taking the cross-correlation with respect to  $u[n]$  of both sides,

$$C_{dy} = h[n] * C_{dd}$$

and assuming that  $C_{dd}$  is an impulse (valid for long sequences), we can obtain the channel impulse response:

$$h[n] = C_{dy}$$

## 2.2 Channel tracking by Recursive least squares (RLS) algorithm

Recursive least squares (RLS) algorithm is used in adaptive filters to find the filter coefficients that relate to recursively producing the least squares (minimum of the sum of the absolute squared) of the error signal (difference between the desired and the actual signal). This is contrast to other algorithms that aim to reduce the mean square error. The difference is that RLS filters are dependent on the signals themselves, whereas MSE filters are dependent on their statistics (specifically, the autocorrelation of the input and the cross-correlation of the input and desired signals). If these statistics are known, an MSE filter with fixed coefficients (i.e., independent of the incoming data)

can be built [4].

First, consider a UWA channel system model shown in figure 2-2. All data processing, analysis, and modeling in this thesis are done with respect to a sampled baseband received signal. Thus all discussion is with respect to discrete time signals and processes. Given the set of input samples  $d(n)$  and the desired response or received signal  $y(n)$ , which is

$$y[n] = \sum_{k=0}^N h_k^* [n]d[n - k] + v[n]$$

$h[n]$  is the baseband complex time-varying channel impulse response,  $N$  is channel length, and  $v(n)$  represents ambient noise. We will attempt to recover the desired signal  $d(n)$  by use of an FIR filter,  $\hat{h}(n)$ .

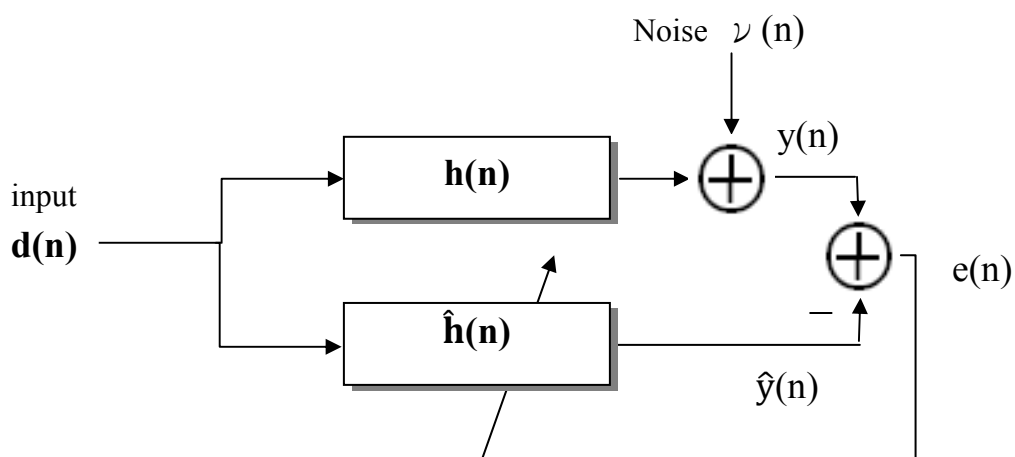
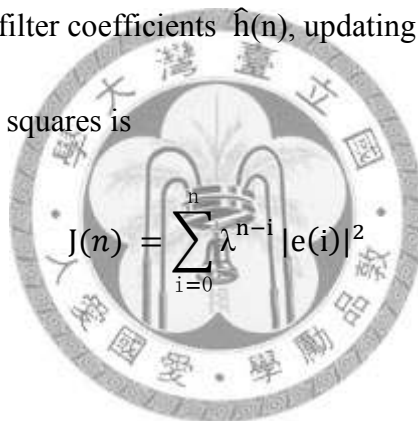


Figure 2-2 Adaptive filter

Our goal is to estimate the parameters of the filter  $\hat{h}$ , and at each time  $n$  we refer to the new least squares estimate by  $\hat{h}(n)$ . As time evolves, we would like to avoid completely redoing the least squares algorithm to find the new estimate for  $\hat{h}(n+1)$ , in terms of  $\hat{h}(n)$ . The benefit of the RLS algorithm is that there is no need to invert matrices, thereby saving computational power. Another advantage is that it provides intuition behind such results as the Kalman filter.

The idea behind RLS filters is to minimize the sum of weighted error squares by appropriately selecting the filter coefficients  $\hat{h}(n)$ , updating the filter as new data arrives. The weighted error squares is



$$J(n) = \sum_{i=0}^n \lambda^{n-i} |e(i)|^2$$

where the error signal is

$$e(i) = y(i) - \sum_{k=0}^N \hat{h}_k^* [n] d[n-k]$$

and the forgetting factor or weighting factor  $\lambda$  ( $0 < \lambda \leq 1$ ) reduces the influence of old data.

The LS solution can be obtained as

$$\hat{h}(n) = \Phi^{-1}(n) z(n)$$

where

$$\Phi(\mathbf{n}) = \sum_{i=1}^n \lambda^{n-i} \mathbf{d}(i) \mathbf{d}(i)^H$$

And

$$\mathbf{z}(\mathbf{n}) = \sum_{i=1}^n \lambda^{n-i} \mathbf{d}(i) y(i)^*$$

We want to find a recursive in time way, so we will rewrite the variables  $\Phi(\mathbf{n})$

and  $\mathbf{z}(\mathbf{n})$  as functions of  $\Phi(\mathbf{n} - 1)$  and  $\mathbf{z}(\mathbf{n} - 1)$ :

$$\Phi(\mathbf{n}) = \lambda \sum_{i=1}^{n-1} \lambda^{n-i-1} \mathbf{d}(i) \mathbf{d}(i)^H + \mathbf{d}(n) \mathbf{d}(n)^H = \lambda \Phi(\mathbf{n} - 1) + \mathbf{d}(n) \mathbf{d}(n)^H$$

$$\mathbf{z}(\mathbf{n}) = \lambda \sum_{i=1}^{n-1} \lambda^{n-i-1} \mathbf{d}(i) y(i)^* + \mathbf{d}(n) y(n)^* = \lambda \mathbf{z}(\mathbf{n} - 1) + \mathbf{d}(n) y(n)^*$$

Applying the matrix inversion formula to  $\Phi(\mathbf{n})$ , we obtain

$$\begin{aligned} \mathbf{P}(\mathbf{n}) &= \Phi^{-1}(\mathbf{n}) \\ &= \lambda^{-1} \Phi^{-1}(\mathbf{n} - 1) - \frac{\lambda^{-2} \Phi^{-1}(\mathbf{n} - 1) \mathbf{d}(n) \mathbf{d}(n)^H \Phi^{-1}(\mathbf{n} - 1)}{1 + \lambda^{-1} \mathbf{d}(n)^H \Phi^{-1}(\mathbf{n} - 1) \mathbf{d}(n)} \end{aligned}$$

Let

$$\mathbf{k}(\mathbf{n}) = \frac{\lambda^{-1} \mathbf{P}(\mathbf{n} - 1) \mathbf{d}(n)}{1 + \lambda^{-1} \mathbf{d}(n)^H \mathbf{P}(\mathbf{n} - 1) \mathbf{d}(n)}$$

Using these definitions, we may rewrite  $\mathbf{P}(\mathbf{n})$  as

$$\mathbf{P}(\mathbf{n}) = \lambda^{-1} \mathbf{P}(\mathbf{n} - 1) - \lambda^{-1} \mathbf{k}(\mathbf{n}) \mathbf{d}(n)^H \mathbf{P}(\mathbf{n} - 1)$$

And we may simplify that

$$\mathbf{k}(\mathbf{n}) = \mathbf{P}(\mathbf{n}) \mathbf{d}(n)$$

We are now able to derive the main time-update equation, that of  $\hat{\mathbf{h}}(n)$

$$\hat{\mathbf{h}}(\mathbf{n}) = \hat{\mathbf{h}}(\mathbf{n}-1) + \mathbf{k}(\mathbf{n}) \zeta^*(\mathbf{n})$$

Where

$$\zeta(\mathbf{n}) = y(\mathbf{n}) - \hat{\mathbf{h}}^H(\mathbf{n}-1) \mathbf{d}(\mathbf{n})$$

Now we can collect all necessary equations to form the RLS algorithm,  $\mathbf{k}(\mathbf{n})$

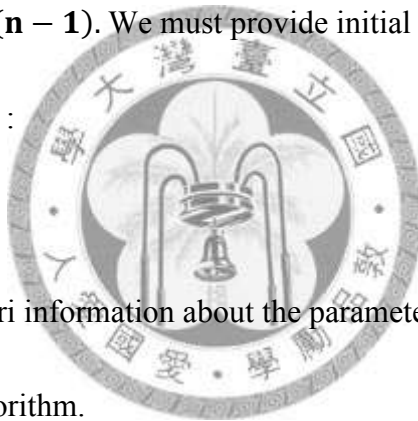
$$\zeta(\mathbf{n}) \quad \hat{\mathbf{h}}(\mathbf{n}) \quad \mathbf{P}(\mathbf{n})$$

Initialization of RLS algorithm:

In RLS algorithm there are two variables involved in the recursions (those with time index  $\mathbf{n}-1$ ):  $\hat{\mathbf{h}}(\mathbf{n}-1)$ ,  $\mathbf{P}(\mathbf{n}-1)$ . We must provide initial values for these variables in order to start the recursions :

•  $\hat{\mathbf{h}}(\mathbf{0})$

If we have some apriori information about the parameters  $\hat{\mathbf{h}}$  this information will be used to initialize the algorithm.



Otherwise, the typical initialization is

$$\hat{\mathbf{h}}(\mathbf{0}) = \mathbf{0}$$

•  $\mathbf{P}(\mathbf{0})$

Recalling the significance of  $\mathbf{P}(\mathbf{n})$

it is not a simple matter to select the length of data required for ensuring invertibility of  $\Phi(\mathbf{0})$ . The approximate initialization is commonly used, it don't require matrix inversion:



$$\mathbf{P}(0) = \delta \mathbf{I}$$

Since our knowledge of these parameters at  $n = 0$  is very vague, a very high covariance matrix of the parameters is to be expected, and thus we must assign a high value to  $\delta$ . The recommended value for  $\delta$  is

$$\delta > 100\sigma_u^2$$

For large data length, the initial values assigned at  $n = 0$  are not important, since they are forgotten due to exponential forgetting factor  $\lambda$ .

Summary of the RLS algorithm:

Given data  $d(1), d(2), d(3), \dots, d(N)$  and  $y(1), y(2), y(3), \dots, y(N)$

1. Initialize  $\mathbf{w}(0)=\mathbf{0}, \mathbf{P}(0)=\delta\mathbf{I}$
2. For each time instant,  $n = 1, \dots, N$ , Compute
  - 2.1  $\boldsymbol{\pi} = \mathbf{u}^H(\mathbf{n})\mathbf{P}(\mathbf{n}-1)$
  - 2.2  $\gamma = \lambda + \boldsymbol{\pi} \mathbf{d}$
  - 2.3  $\mathbf{k}(\mathbf{n}) = \frac{\boldsymbol{\pi}}{\gamma}$
  - 2.4  $\zeta(n) = y(n) - \hat{\mathbf{h}}^H(\mathbf{n}-1)d(n)$
  - 2.5  $\hat{\mathbf{h}}(\mathbf{n}) = \hat{\mathbf{h}}(\mathbf{n}-1) + \mathbf{k}(\mathbf{n})\zeta^*(n)$
  - 2.6  $\mathbf{P}' = \mathbf{k}(\mathbf{n})\boldsymbol{\pi}$
  - 2.7  $\mathbf{P}(\mathbf{n}) = \frac{1}{\lambda}(\mathbf{P}(\mathbf{n}-1) - \mathbf{P}')$

## 2.3 The impact of channel estimation error on the equalizer

In this section, we will discuss the impact of channel estimation error on the channel estimation based equalizers.

First, consider the channel and equalizer model. Again, all data processing, analysis, and modeling in this thesis are done with respect to a sampled baseband received signal. Thus all discussion is with respect to discrete time signals and processes. The acoustic channel is modeled as a time-varying, discrete time system described by the complex baseband time-varying impulse response. (see Proakis[11] and Van Trees[12]). The received signal at time  $n$  is given by

$$y[n] = \sum_{m=-N_a}^{N_c-1} h_m^*[n]d[n-m] + v[n]$$

This relation also shown in the figure 2-3

where  $h[n]$  is the baseband complex time-varying channel impulse response relating the input signal at time  $(n-m)$  to the output signal at time  $n$ ,  $d[n]$  is the complex baseband transmitted data, and  $v[n]$  is complex baseband observation noise. The quantities  $N_a$  and  $N_c$  denote, respectively, the number of acausal and causal taps in the channel impulse response.

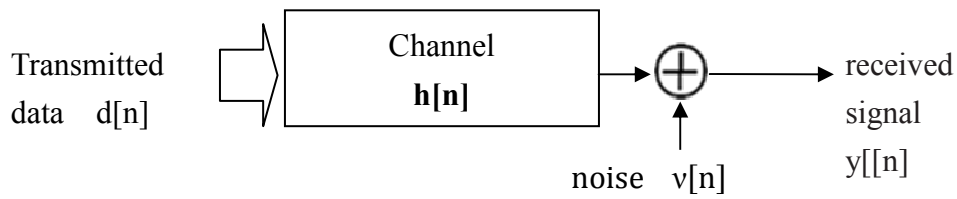


Figure 2-3 system model

And the performance of channel estimation based equalizers is characterized in terms of the mean squared soft decision error  $\sigma_s^2$  of each equalizer [13]. Figure 2-4 shows a channel estimate based decision feedback equalizer (CE-DFE), and Figure 2-5 shows a linear equalizer. The received signal  $y[n]$ , is processed to generate estimates of the time-varying impulse response of the channel between the transmitter and each receive hydrophone. The impulse response estimates are used to compute the equalizer filter weights. These filter weights are used to implement the equalizer and estimate the desired data symbol  $d[n]$ . Then we can define the soft decision error

$$\epsilon_s = \hat{d}_s[n] - d[n].$$

Furthermore, the mean squared soft decision error  $\sigma_s^2$  can be decomposed into two components. These are the minimum achievable error ( $\sigma_0^2$ ) and the excess error ( $\sigma_\epsilon^2$ ) [13].

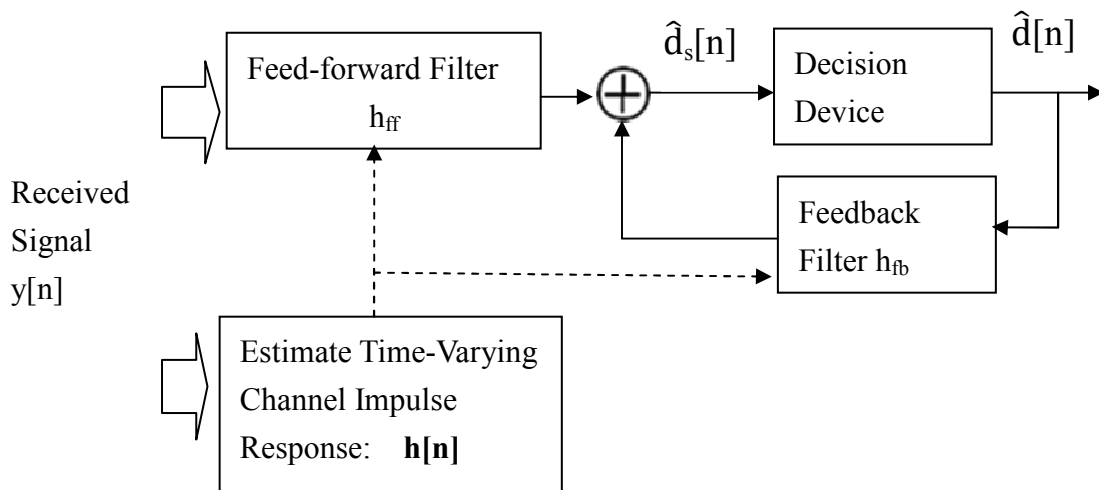


Figure 2-4 CE-DFE

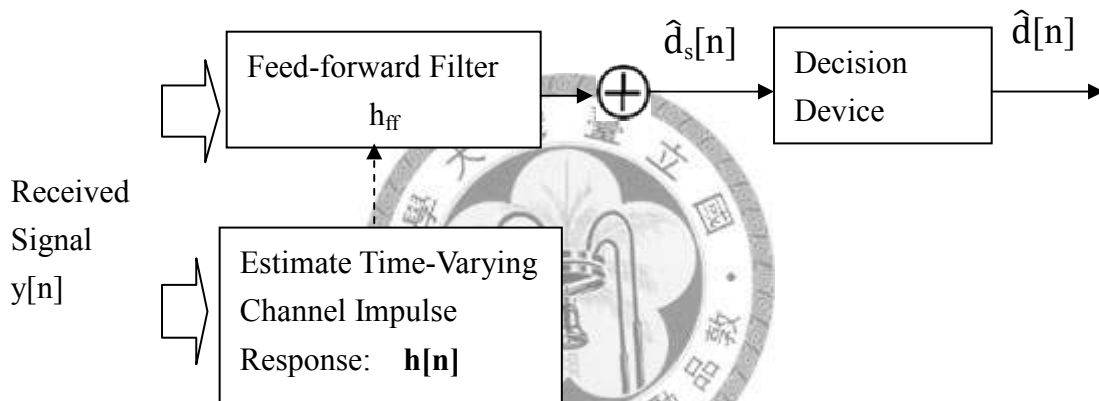


Figure 2-5 linear equalizer

The minimum achievable error  $\sigma_0^2$  is the soft decision error that would be realized by the equalizer if the filter coefficient calculation were based upon perfect knowledge of the channel impulse response and statistics of the interfering noise field.

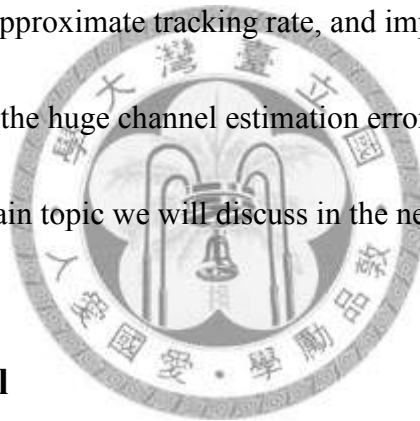
And the excess error ( $\sigma_e^2$ ) is the additional soft decision error that is realized due to errors in the estimates of these channel parameters.

They separately quantify the equalizer errors here that leads to new insights into

the factors that can limit equalizer performance and the characteristics of equalizers that are robust with respect to channel estimation errors.

The finally analysis of experimental data verifies that the expressions can accurately predict equalizer performance when the second-order statistics of the errors in the channel impulse response estimates are known. And they also show that the excess error was always a significant contributor to the soft decision error when rough sea conditions prevailed.

So we should set the approximate tracking rate, and improve the accuracy of channel estimation further, the huge channel estimation error will degrade the equalizer performance. This is the main topic we will discuss in the next two sections.



## 2.4 AR channel model

When the transmission medium became time-varying cause of internal wave, ambient noise, or some unexpected situation, the adaptive filtering algorithm now has the added task of tracking the time-varying environment.

Tracking is a steady-state phenomenon, to be contrasted with convergence, which is a transient phenomenon. it follows that, for an adaptive filter to exercise its tracking capability, it must first pass from the transient mode to the steady-state mode of operation, and there must be provision for continuous adjustment of the free

parameters of the filter.

A popular approach for this analytical assessment is to assume a first-order AR model, Although higher-order models are also possible, only a few results on the tracking performance using these models are currently available, In our analysis of tracking characteristics of the adaptive algorithms, we use the first-order AR model. This setup is illustrated in Figure 2-6.

The tap-weight vector  $\mathbf{h}(n)$  represents the “target”(real channel) to be tracked by the filter. In the ASIAEX experiment ,we can get this by pulse compression using m-sequence property.

$\hat{\mathbf{h}}(n)$  is the tap-weight vector of the adaptive filter. whenever  $\hat{\mathbf{h}}(n)$  equals  $\mathbf{h}(n)$ ,the minimum mean-square error produced by the adaptive filter equals the irreducible error variance  $\sigma^2$ .



Desired response:

$$y(n) = \mathbf{h}^H(n)\mathbf{d}(n) + v(n)$$

And  $v(n) = y(n) - \mathbf{h}^H(n)\mathbf{d}(n)$

The variation of channel  $\mathbf{h}(n)$  is modeled by the first-order AR (or Markov) process:

$$\mathbf{h}(n + 1) = \rho \mathbf{h}(n) + \Psi(n)$$

Where,  $\rho = e^{-\omega_d T}$  ,and  $\omega_d$  is Doppler spread [14]

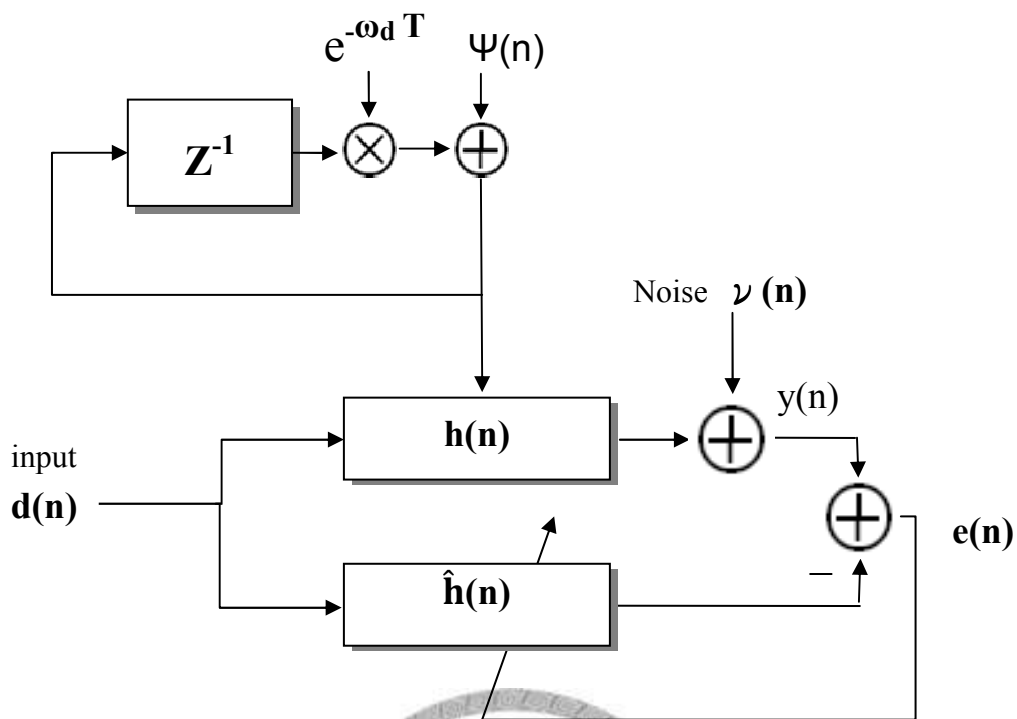


Figure 2-6 AR model

Tracking is generally achievable if  $\rho$  is close to 1. The random-walk model is obtained by using  $\rho = 1$ .

To determine whether an adaptive algorithm can adequately track the changing SOE(signal operating environment), one needs to define the speed of variation of the statistics of the adaptive filter environment. This speed is quantified in terms of the degree of nonstationarity (DNS), introduced in Macchi [15], and is defined by:

$$\eta(n) = \sqrt{\frac{E[|\Psi^H(n)\mathbf{d}(n)|^2]}{E[|\nu[n]|^2]}}$$

where,  $\Psi(n) = \mathbf{h}(n) - \rho \mathbf{h}(n-1)$

Smaller values of  $\eta$  ( $\ll 1$ ) imply that the adaptive algorithm can track time variations of the nonstationary SOE. On the contrary, if  $\eta > 1$ , then the statistical variations of the adaptive filters SOE are too fast for the adaptive algorithm to keep up with the SOE and lead to massive misadjustment errors. In such situations, an adaptive filter should not be used.

It won't be surprised that DNS directly correlate with the optimal forgetting factor:

## 2.5 The optimal forgetting factor of RLS

The performance of adaptive FIR filters governed by the recursive least-squares (RLS) algorithm are done in terms of the steady-state excess mean-square estimation error  $\delta$  and the steady-state mean-square weight deviation  $\zeta$ [16].

Let  $\hat{\mathbf{h}}_k$ ,  $\mathbf{d}_k$ ,  $v_k$  and  $y_k$  denote the weight vector of the adaptive filter at discrete time  $k$ , the observation vector, observation noise, and the desired filter output, respectively.

The estimation error  $e_k$  is given by:

$$e_k = y_k - \hat{\mathbf{h}}_k^H \mathbf{d}_k$$

The steady-state excess mean-square estimation error  $\delta$  is defined by

$$\delta \triangleq \lim_{k \rightarrow \infty} |e_k|^2 - \sigma_v^2$$



The steady-state mean-square weight deviation  $\zeta$  is defined by

$$\zeta \triangleq \lim_{k \rightarrow \infty} \|\hat{\mathbf{h}}_k - \mathbf{h}_k\|$$

The value of  $\lambda$  that minimizes  $\zeta$ , and the minimum value of  $\zeta$ , are, respectively,

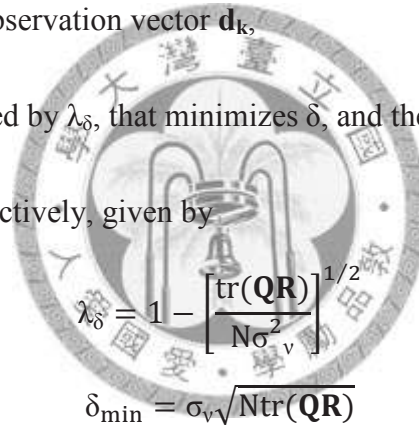
given by:

$$\lambda_\zeta = 1 - \left[ \frac{\text{tr}(\mathbf{Q})}{\sigma_v^2 \text{tr}(\mathbf{R}^{-1})} \right]^{1/2}$$

$$\zeta_{\min} = \sigma_v \sqrt{\text{tr}(\mathbf{Q}) \text{tr}(\mathbf{R}^{-1})}$$

Where  $\mathbf{Q}$  is the covariance matrix of the channel increments  $\mathbf{d}_{k+1} - \mathbf{d}_k$ , and  $\mathbf{R}$  is the covariance matrix of the observation vector  $\mathbf{d}_k$ .

The value of  $\lambda$ , denoted by  $\lambda_\delta$ , that minimizes  $\delta$ , and the minimum value of  $\delta$ , denoted by  $\delta_{\min}$ , are, respectively, given by



$$\lambda_\delta = 1 - \left[ \frac{\text{tr}(\mathbf{QR})}{N\sigma_v^2} \right]^{1/2}$$

$$\delta_{\min} = \sigma_v \sqrt{N \text{tr}(\mathbf{QR})}$$

In this thesis, we are focus on the accuracy of channel estimation, so the weight deviation is the primary performance index. In the particular case when  $\mathbf{R} = c\mathbf{I}$ , the values of forgetting factor  $\lambda$  that minimizes  $\delta$  or  $\zeta$  are exactly the same. However, the transmitted bits are practically uncorrelated with each other.

## Chapter 3 Optimal forgetting factor estimation

The performance of adaptive FIR filters governed by the recursive least-squares (RLS) algorithm is considered into two metrics, one is the steady-state excess mean-square estimation error  $\delta$  and the other one is the steady-state mean-square weight deviation  $\zeta$ . In this thesis, we are focus on the accuracy of channel estimation, so the weight deviation is the primary performance index. For many times, the values of forgetting factor  $\lambda$  that minimizes  $\delta$  or  $\zeta$  are exactly the same, it can be easily observed in ASIAEX experiment data shown in figure 3-1(the experiment environment will be introduced in section 4).

In the following sections, we will discuss all the parameters that the  $\lambda_{\text{opt}}$  needed, for instance, the innovation  $\Psi$ , Doppler spread  $\omega_d$ , observation noise  $\nu$ , etc.

### 3.1 Implementation of forgetting factor estimation

The value of forgetting factor that minimizes the steady-state mean-square weight deviation  $\zeta$  of RLS algorithm can be obtained by:

$$\zeta \triangleq \lim_{k \rightarrow \infty} E(\|\mathbf{h}_k - \hat{\mathbf{h}}_{k,\lambda}\|^2)$$
$$\lambda_{\text{opt}} = \arg \min_{\lambda} \lim_{k \rightarrow \infty} E(\|\mathbf{h}_k - \hat{\mathbf{h}}_{k,\lambda}\|^2)$$

where  $\mathbf{h}_k$  is real acoustic channel impulse response, and  $\hat{\mathbf{h}}_{k,\lambda}$  is tap weight

vector measured by RLS for forgetting factor  $\lambda$ , an example is shown in figure 3-1.

And the theoretical value of forgetting factor that minimizes the  $\zeta$  is mentioned in section 2.5, is given by:

$$\lambda_{\text{opt}} = 1 - \left[ \frac{\text{tr}(\mathbf{R}_{\Psi})}{\sigma_v^2 \text{tr}(\mathbf{R}_d^{-1})} \right]^{1/2}$$

Assume that each tap of  $\Psi$  and  $d$  are uncorrelated, and  $\Psi$  and  $d$  are also uncorrelated, we can get that:

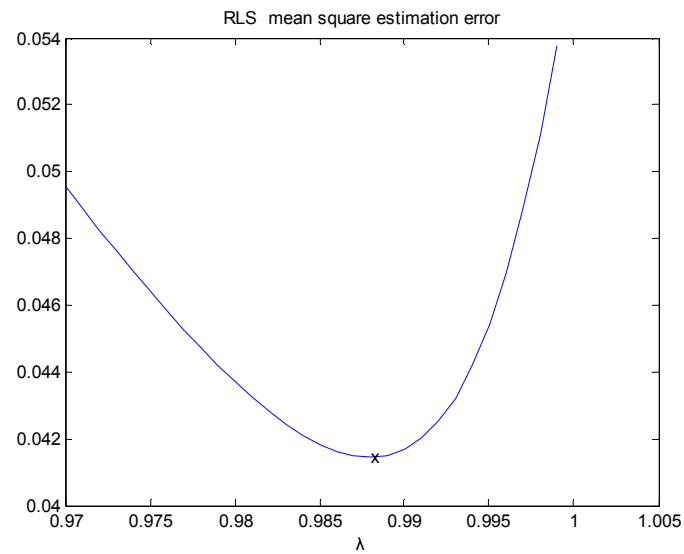
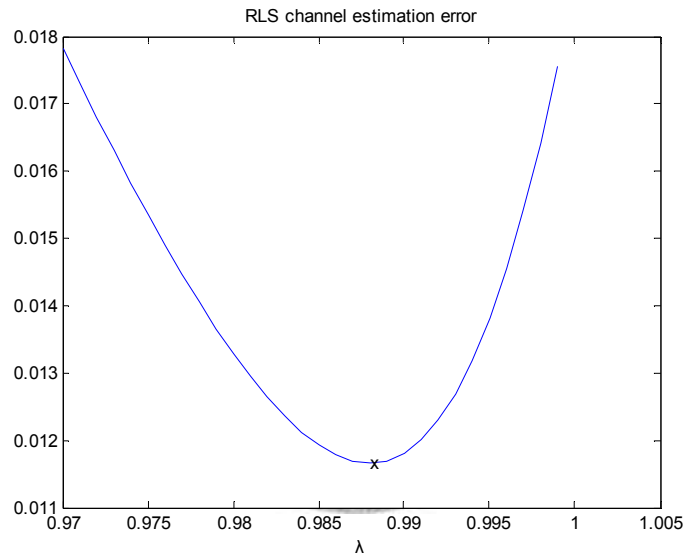


Figure 3-1 optimal forgetting factor for ASIAEX data-day 126-6:15:32 (channel 16)

$$\lambda_{\text{opt}} = 1 - \left[ \frac{\text{tr}(\mathbf{R}_{\Psi} \mathbf{R}_{\mathbf{d}})}{N\sigma_v^2} \right]^{1/2}$$

where  $N$  is the dimension of input signal vector  $\mathbf{d}$ , and

$$\begin{aligned} \text{tr}(\mathbf{R}_{\Psi} \mathbf{R}_{\mathbf{d}}) &= \text{tr}\{\mathbf{E}[\boldsymbol{\Psi}(n)\boldsymbol{\Psi}^H(n)]\mathbf{E}[\mathbf{d}(n)\mathbf{d}^H(n)]\} \\ &= \mathbf{E}\{\text{tr}[\boldsymbol{\Psi}(n)\boldsymbol{\Psi}^H(n)\mathbf{d}(n)\mathbf{d}^H(n)]\} \\ &= \text{tr}\{\mathbf{E}[\boldsymbol{\Psi}^H(n)\mathbf{d}(n)\mathbf{d}^H(n)\boldsymbol{\Psi}(n)]\} \\ &= \mathbf{E}[\boldsymbol{\Psi}^H(n)\mathbf{d}(n)\mathbf{d}^H(n)\boldsymbol{\Psi}(n)] \\ &= \mathbf{E}[|\boldsymbol{\Psi}^H(n)\mathbf{d}(n)|^2] \end{aligned}$$

So the equation of  $\lambda_{\text{opt}}$  can be reformed to:

$$\lambda_{\text{opt}} = 1 - \left[ \frac{\mathbf{E}[|\boldsymbol{\Psi}^H(n)\mathbf{d}(n)|^2]}{N\sigma_v^2} \right]^{1/2}$$

And recall the degree of nonstationarity (DNS) mentioned in section 2.4, we can easily correlate the  $\lambda_{\text{opt}}$  with DNS:

$$\lambda_{\text{opt}} = 1 - \frac{\eta}{\sqrt{N}}$$

In order to calculate the DNS at the beginning of a data packet transmission period, we should add some bits consisted of “maximum length sequence” in front of the data bits, which is shown in Figure 3-2.  $N$  is the number of slots in the shift register, also called the order of the m-sequence. Thus an order  $N=6$  means a sequence with a period of 63 samples. Consider the long multipath delay time of underwater acoustic channel,  $N$  should be chosen enough large to guarantee that able to calculate the

channel impulse response accurately.  $M$  is additional bits, in order to obtain sufficient statistics and measure the DNS further.

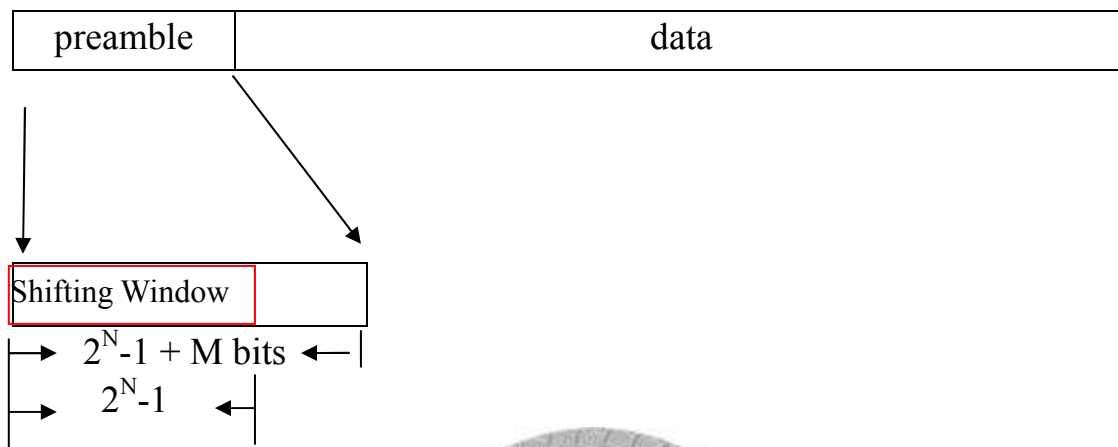
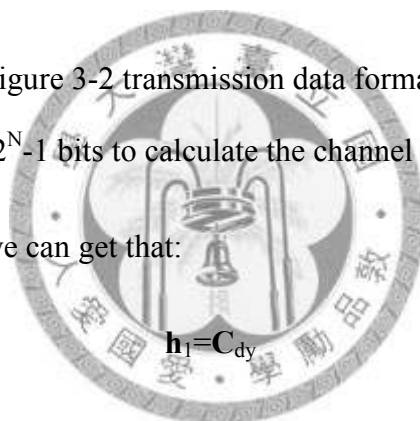


Figure 3-2 transmission data format

First, we use the first  $2^N - 1$  bits to calculate the channel impulse response, as mentioned in section 2.1, we can get that:



$$\mathbf{h}_1 = C_{dy}$$

Where  $C$  is cross-correlation function,  $\mathbf{d}[n]$  is transmitted m-sequence and  $\mathbf{y}[n]$  is received data.

The next step is to shift the window to right for 1 bit, and calculate the second impulse response  $\mathbf{h}_2$  as shown in Figure 3-3.

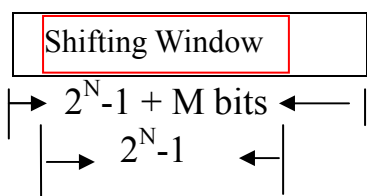


Figure 3-3 window shift one bit

Follow M+1 times the above-mentioned step, we can get  $h_k$  for  $k=1$  to  $M+1$ .

And recalling the AR model of section 2.4, as follows

The innovation  $\Psi$  is:

$$\Psi_k = \mathbf{h}_{k+1} - \rho \mathbf{h}_k \quad , \text{ for } k=1,2,\dots,M$$

And in matrix form:

$$\begin{bmatrix} \Psi_{k,-Na} \\ \Psi_{k,-Na+1} \\ \vdots \\ \Psi_{k,Nc-1} \end{bmatrix} = \begin{bmatrix} h_{k+1,-Na} \\ h_{k+1,-Na+1} \\ \vdots \\ h_{k+1,Nc-1} \end{bmatrix} - \rho \begin{bmatrix} h_{k,-Na} \\ h_{k,-Na+1} \\ \vdots \\ h_{k,Nc-1} \end{bmatrix}$$

Where,  $\rho = e^{-\omega_d T}$

$\omega_d$  is Doppler spread bandwidth and can be obtained via scattering function will be introduced in next section. The quantities  $N_a$  and  $N_c$  denote, respectively, the number of acausal and causal taps in the channel impulse response.

The observation noise

$$v_k = y_k - \mathbf{h}_k^H \mathbf{d}_k \quad , \text{ for } k=2,\dots,M+1$$

Finally, the degree of nonstationarity:

$$\eta = \sqrt{\frac{E[|\Psi_k^H \mathbf{d}_k|^2]}{E[|v_k|^2]}} \quad , \text{ for } k=2,\dots,M$$

and

$$\lambda_{\text{opt}} = 1 - \frac{\eta}{\sqrt{N}}$$

Where ,  $y_{k,\text{incr}} = \Psi_k^H \mathbf{d}_k$  is the output of the incremental filter, and  $N = N_a + N_c$

### 3.2 Doppler-Spread estimation

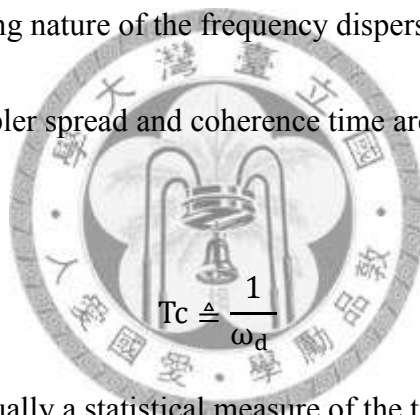
For waves that propagate in a medium, such as sound waves, the velocity of the observer and of the source are relative to the medium in which the waves are transmitted. The total Doppler effect may therefore result from motion of the source, motion of the observer, or motion of the medium.

Delay spread and coherence bandwidth are parameters which describe the time dispersive nature of the channel in a local area. However, they do not offer information about the time varying nature of the channel caused by either relative motion between the mobile and base station, or by movement of objects in the channel. Doppler spread and coherence time are parameters which describe the time varying nature of the channel in a small-scale region.

Doppler spread  $\omega_d$  is a measure of the spectral broadening caused by the time rate of change of the channel and is defined as the range of frequencies over which the received Doppler spectrum is essentially non-zero. When a pure sinusoidal tone of frequency  $f_c$  is transmitted, the received signal spectrum, called the Doppler spectrum,

will have components in the range  $f_c - f_d$  to  $f_c + f_d$ , where  $f_d$  is the Doppler shift. The amount of spectral broadening depends on  $f_d$  which is a function of the relative velocity of the mobile, and the angle  $\theta$  between the direction of motion of the mobile and direction of arrival of the scattered waves. If the baseband signal bandwidth is much greater than  $\omega_d$  the effects of Doppler spread are negligible at the receiver. This is a slow fading channel.

Coherence time  $T_c$  is the time domain dual of Doppler spread and is used to characterize the time varying nature of the frequency dispersiveness of the channel in the time domain. The Doppler spread and coherence time are inversely proportional to one another. That is,



$$T_c \triangleq \frac{1}{\omega_d}$$

Coherence time is actually a statistical measure of the time duration over which the channel impulse response is essentially invariant, and quantifies the similarity of the channel response at different times. In other words, coherence time is the time duration over which two received signals have a strong potential for amplitude correlation. If the reciprocal bandwidth of the baseband signal is greater than the coherence time of the channel, then the channel will change during the transmission of the baseband message, thus causing distortion at the receiver.

A Doppler spread for a communications channel is measured by providing an



estimate of the communications channel and doing Fourier transform along the time domain for the estimate of the communications channel  $\hat{h}$ , which can be calculated by some methods mentioned in section 2. The formula expression is shown below and  $\mu$  is called delay Doppler spread function:

$$\mu[l, k] = \sum_{i=1}^L \hat{h}[i, k] e^{-j2\pi v_l i \Delta t}$$

Here,  $\hat{h}[i, k] \triangleq h(i\Delta t, \tau_k)$ ,  $\tau_k \triangleq \tau_0 + (k - 1)\Delta\tau$  for  $k=1, \dots, K$  are the sampled delays,  $\tau_0$  is the reference delay.  $\Delta t$  and  $\Delta\tau$  are the sample intervals in time and delay.  $K$  is the number of uniformly sampled delay taps, i.e., the channel dimension.

And  $\mu[l, k] \triangleq \mu(v_l, \tau_k)$ ,  $v_l \triangleq v_0 + (l - 1)\Delta v$  for  $l=1, \dots, L$  are the sampled Dopplers with  $v_0$  and  $\Delta v$  as the reference Doppler and the Doppler sample interval, respectively.

If  $\mu[l, k]$  is WSSUS, the scattering function can be expressed as

$$P[l, k] = E\{\mu[l, k]\}^2$$

And the other way to obtain the scattering function is that correlating a portion of a received signal with the bank of Doppler-shifted replicas of the transmitted m-sequence .

Here is some example shown in Figure 3-4 to Figure 3-7, the data is based on ASIAEX experiment, which will be introduced in section 4. Figure 3-4 shows the

channel impulse response in time domain and delay domain, and the corresponding delay Doppler spread function shown in Figure 3-5.

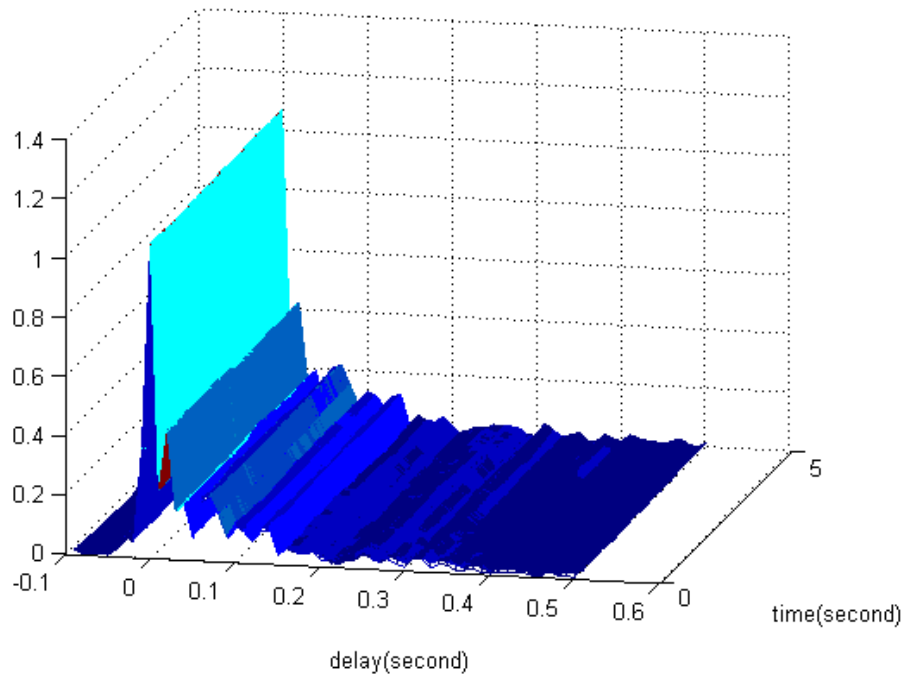
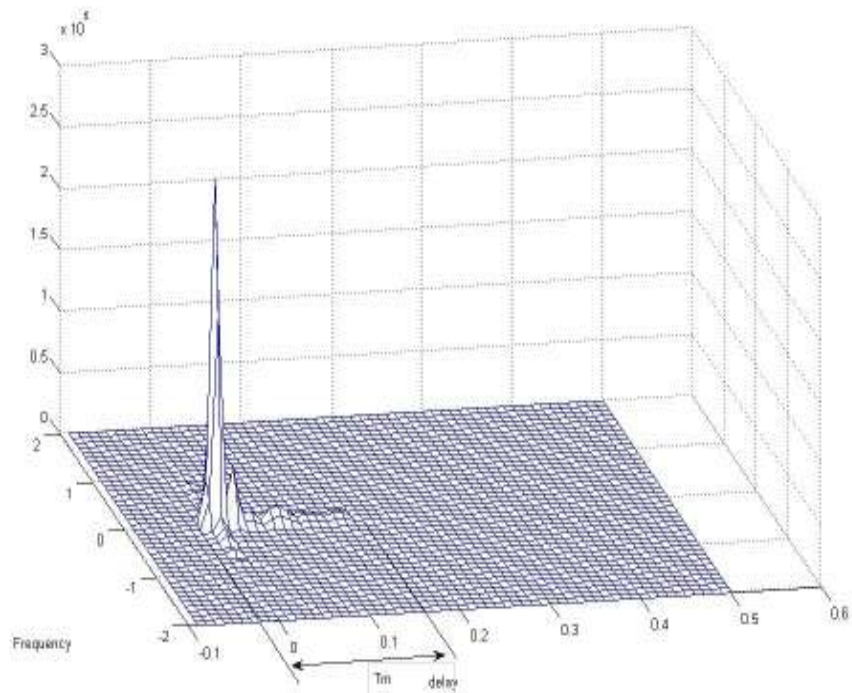


Figure 3-4 channel impulse response in time domain and delay domain for ASIAEX –day 126-6:15:17 (channel 16)



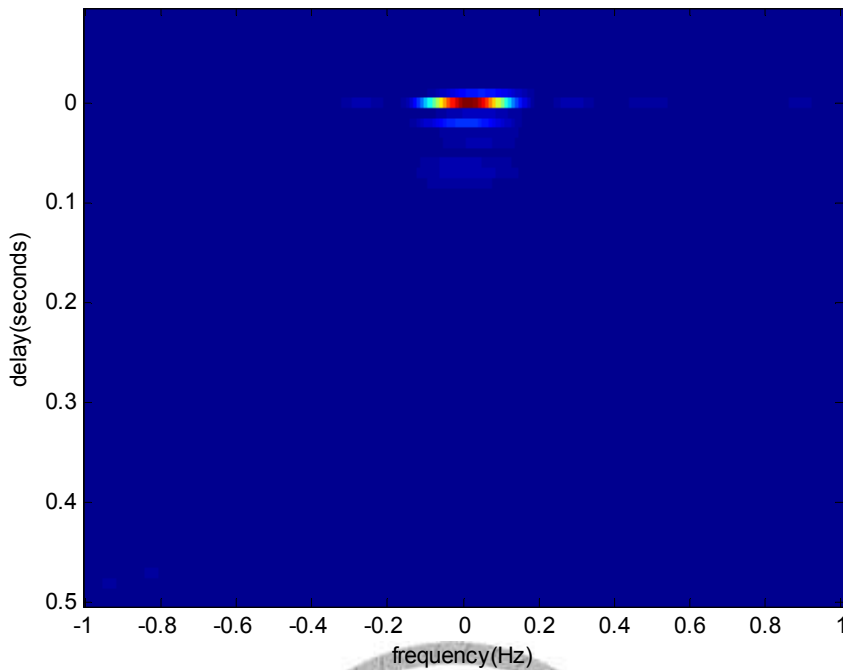


Figure 3-5 The scattering function of ASIAEX –day 126-6:15:17 (channel 16)

Where the value  $T_m$  is called “multipath spread” and the correspond “coherence bandwidth” is:

$$(\Delta f)_c \triangleq \frac{1}{T_m}$$

And for direct path, we can calculate the Doppler spread  $\omega_d$  (3db bandwidth) as shown in Figure 3-6.

Now we can observe the difference of delay Doppler spread function between the calm-water channel shown above and the internal-wave-affected channel shown in figure 3-7. it’s obviously that the delay spread and the Doppler spread is growing worse in rough sea condition.

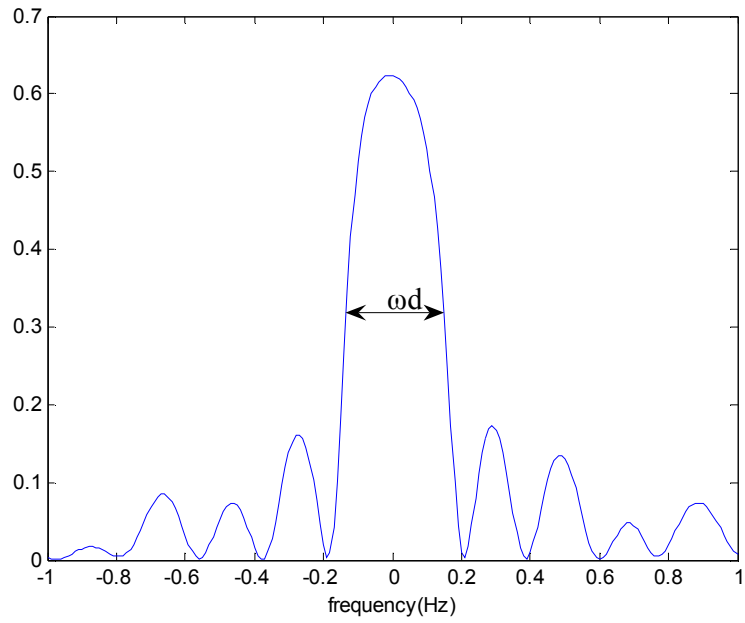
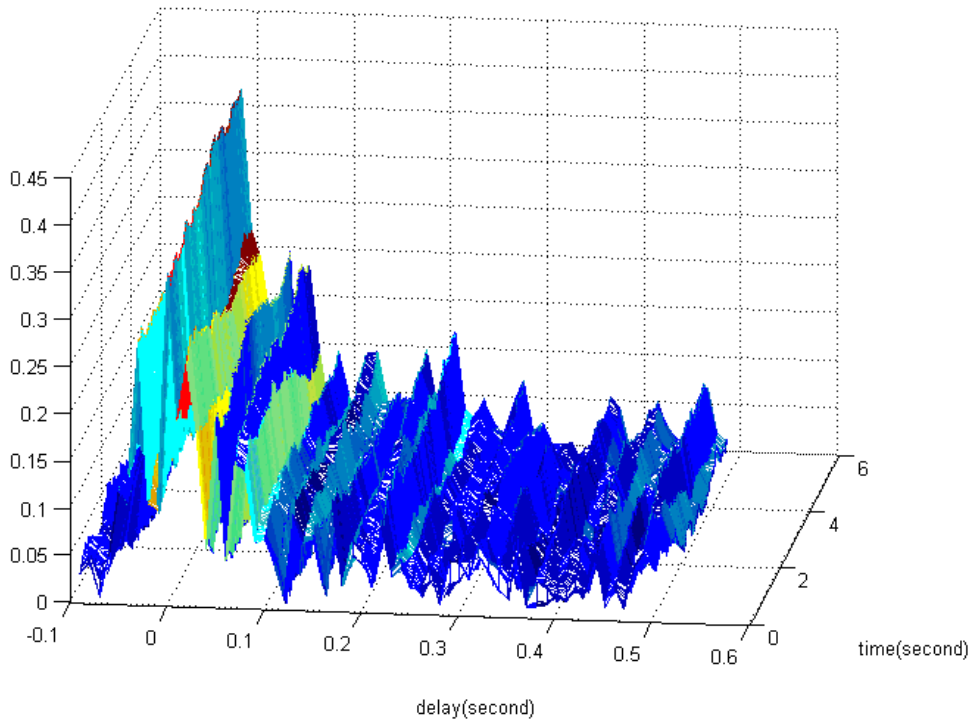
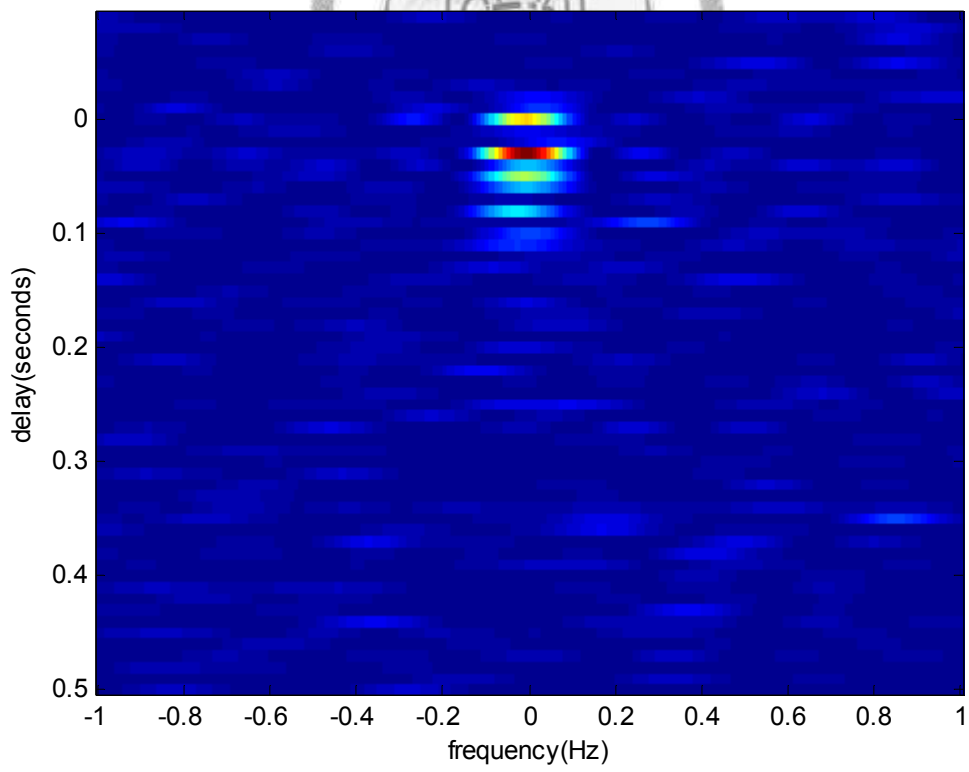
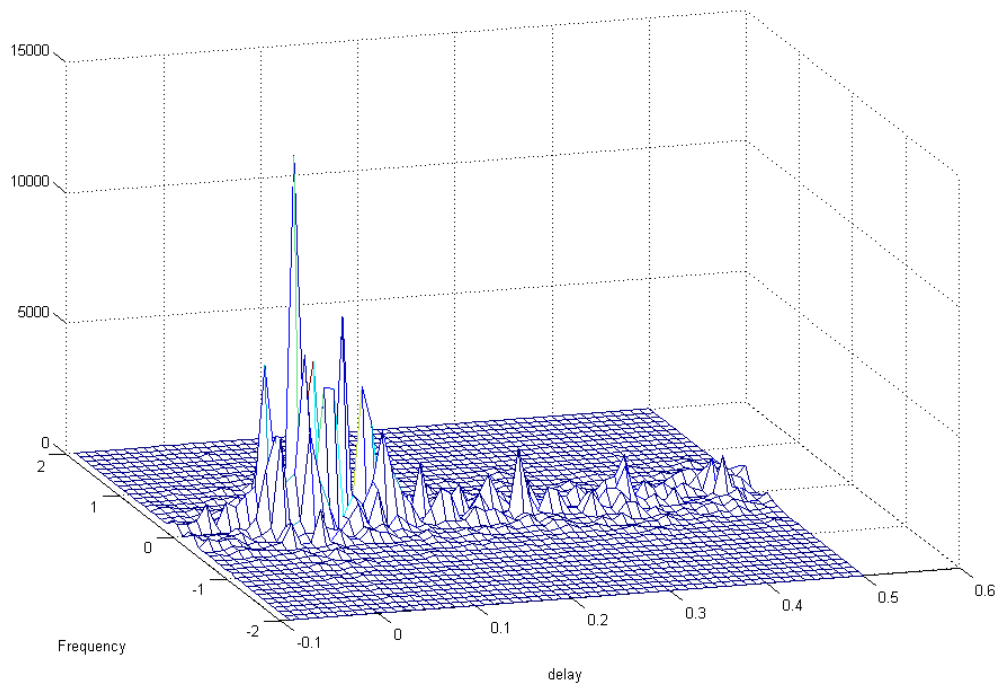


Figure 3-6 The direct-path spectrum of ASIAEX -day 126-6:15:17 (channel 16)





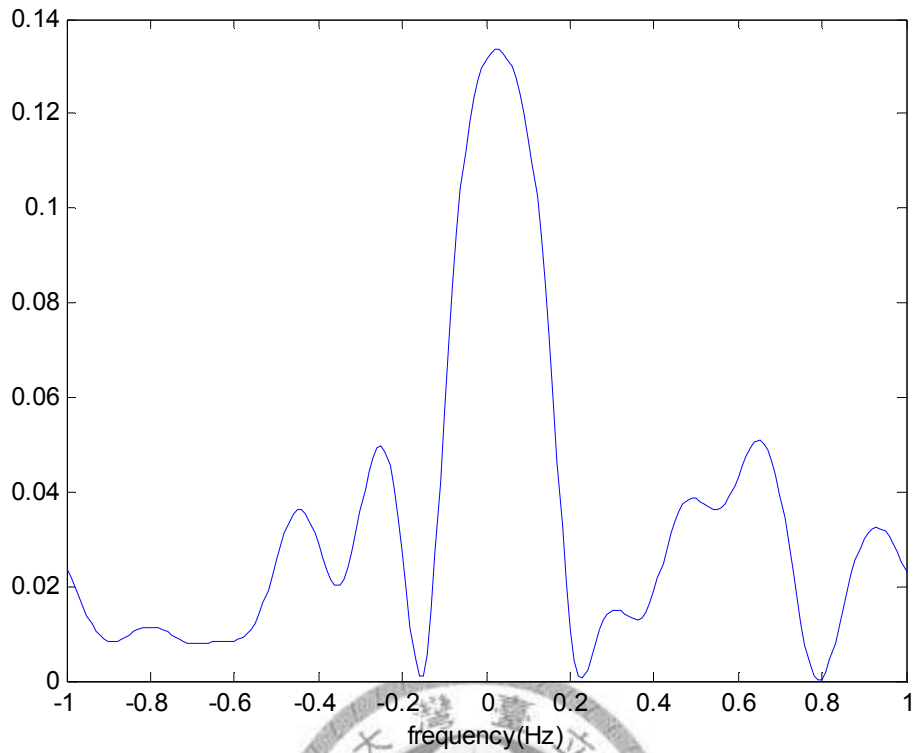


Figure 3-7 The scattering function and the direct path spectrum of ASIAX  
-128\_12\_49\_24\_3937.mat (channel 16)

### 3.3 Compute the approximate optimal forgetting factor

In section 3.1, we discussed how to find optimal forgetting factor  $\lambda$  of RLS, however, this implementation via “degree of nonstationarity” calculating, which suffers very high computational complexity. To reduce the computational complexity by some simplification assumption is necessary. Recall the first order AR process of time-varying channel:

$$\mathbf{h}_{k+1,i} = \rho \mathbf{h}_{k,i} + \Psi_{k,i} \quad \text{for each tap } i=1,2,\dots,N \quad \text{at time } k$$

Where,  $\rho = e^{-\omega_d T}$

Assuming  $\mathbf{h} = \mathbf{h}' - \bar{\mathbf{h}}$ , i.e., assuming the mean of the process has been removed so that  $\bar{\mathbf{h}} = 0$ . Rearranging the model, we get

$$\Psi_k = \mathbf{h}_{k+1} - \rho \mathbf{h}_k$$

In order to avoid any confusing, the notation “i” had been removed.

we next use this formula to estimate the innovation variance by taking the product of the above equation with itself, and taking expectance,

$$\begin{aligned} E[\Psi_k \Psi_k] &= E[\mathbf{h}_{k+1} \mathbf{h}_{k+1}] - 2\rho E[\mathbf{h}_{k+1} \mathbf{h}_k] + \rho^2 E[\mathbf{h}_k \mathbf{h}_k] \\ &= E[\mathbf{h}_k \mathbf{h}_k] - 2\rho E[\mathbf{h}_{k+1} \mathbf{h}_k] + \rho^2 E[\mathbf{h}_k \mathbf{h}_k] \end{aligned}$$

where we have used the fact  $E[\mathbf{h}_k \mathbf{h}_k] = E[\mathbf{h}_j \mathbf{h}_j]$  for any k and j.

then we get that:

$$\sigma_\Psi^2 = c_0 - 2\rho r_1 + \rho^2 c_0$$

where  $\sigma_\Psi^2$  is the expected variance of the innovation,  $r_1$  is the first autocorrelation coefficient, and  $c_i$  is the  $i$ th autocovariance coefficient (so that  $c_0 = \sigma_h^2$ , the sample estimated variance of  $\mathbf{h}$ ). Finally, recall that for AR(1),  $\rho = r_1$ , so

$$\sigma_\Psi^2 = \sigma_h^2 (1 - 2\rho^2 + \rho^2) = \sigma_h^2 (1 - \rho^2)$$

Again, recall the formula for  $\lambda_{\text{opt}}$  :

$$\lambda_{\text{opt}} = 1 - \sqrt{\frac{\text{tr}\{\mathbf{R}_\Psi \mathbf{R}_d\}}{N\sigma_v^2}}$$

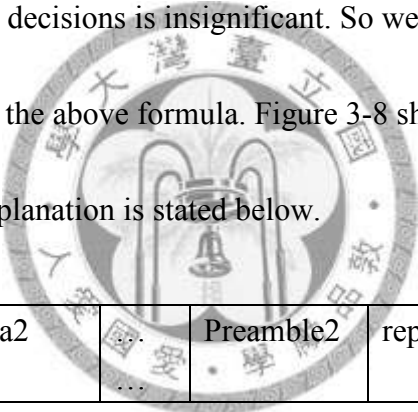
Assuming each tap of  $\Psi$  and  $d$  are uncorrelated, and  $\Psi$  and  $d$  are also uncorrelated,

so this formula can be reformed:

$$\lambda_{\text{opt}} = 1 - \sqrt{\frac{\sum_{i=1}^N \{\sigma_{\Psi,i}^2 \times \sigma_{d,i}^2\}}{N\sigma_v^2}}$$

$$= 1 - \sqrt{\frac{\sum_{i=1}^N \sigma_{h,i}^2 (1 - \rho^2) \times \sigma_{d,i}^2}{N\sigma_v^2}}$$

Suppose that the impact of the decay in the quality of the channel estimate resulting from using incorrect signal decisions in the estimation algorithm or the feedback of incorrect signal decisions is insignificant. So we can roughly estimate the optimal forgetting factor by the above formula. Figure 3-8 shows the transmission packet format, and some explanation is stated below.



Preamble1	data1	data2	...	Preamble2	repeat
-----------	-------	-------	-----	-----------	--------

Preamble1: precisely compute the optimal forgetting factor, denoted  $\lambda_1$

Data1: channel estimation by RLS using  $\lambda_1$ , and calculate  $\sigma_{h,i}$  for each tap and  $\sigma_d$  in the end of this section transmission, finally estimate the approximate optimal forgetting factor, denoted  $\lambda_2$

Data2: channel estimation by RLS using  $\lambda_2$ .

Preamble2: re-compute the precise optimal forgetting factor, and follow the above steps.

Figure 3-8 transmission format



## Chapter4 Experiment Result

The experiment performance is based on ASIAEX data, which will be introduced in section 4.1. In section 4.2 a metrics, SMR, was introduced to reflect the quality of channel. Finally, the performance result discussed in section 4.3 is presented together with the experiment value, and the prediction value of optimal forgetting factor, and of channel estimation mean square error.

### 4.1 The Asian Seas International Acoustics Experiment (ASIAEX)

Between late April and May 23, 2001, a suite of acoustic and oceanographic sensors was deployed by a team of U.S., Taiwan, and Singapore scientists in the northeastern South China Sea [17].



A side view of the relevant portion of the experiment and associated physical parameters are shown in Fig. 4-1.

Moored at 13m above the 350-m isobaths on the slope the sound source transmitted binary phase-shift keying (BPSK) signals at a carrier frequency of 400 Hz with a bandwidth of 100 Hz. The phase modulation employed was a 5.11-s-long 511-digit m-sequence resulting in a compressed pulse of 10-ms resolution after matched filtering. These bihourly transmissions were sampled at a rate of 3.2 kHz by

the vertical hydrophone array moored at the 125-m isobath on the shelf. This listening array consisted of 16 hydrophones moored vertically in the water column, and array has an aperture of 79m spanning the depths from 42 to 121 m.

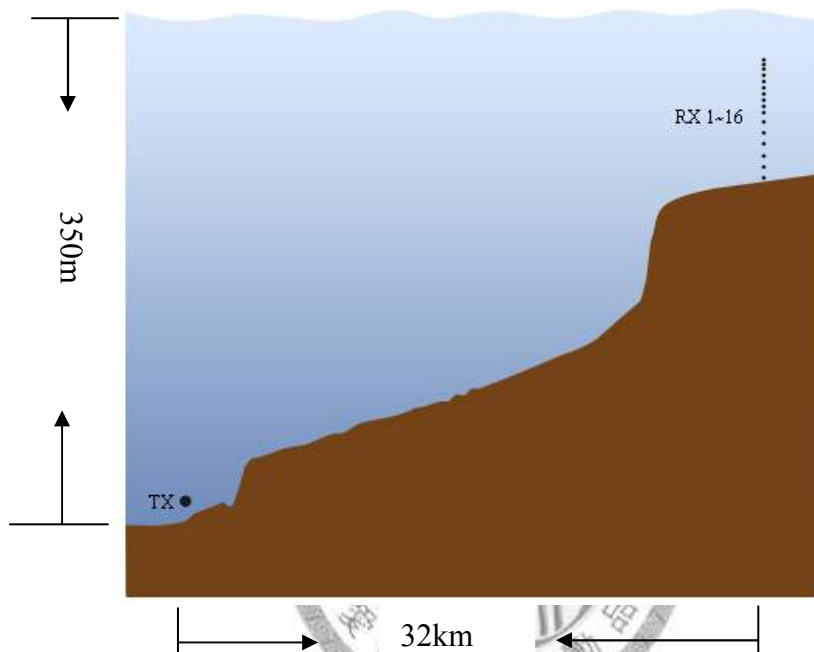
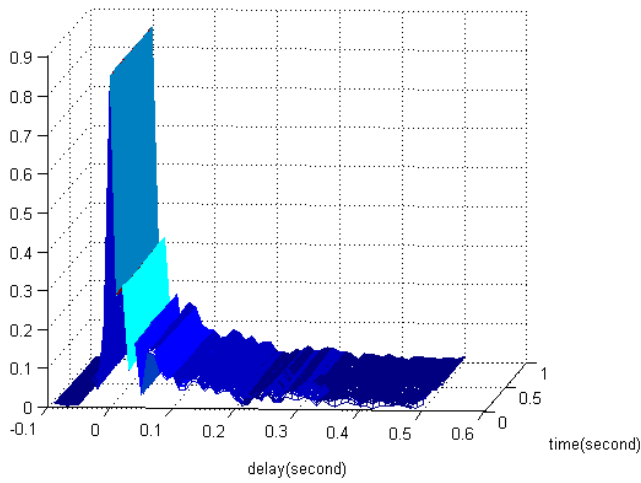


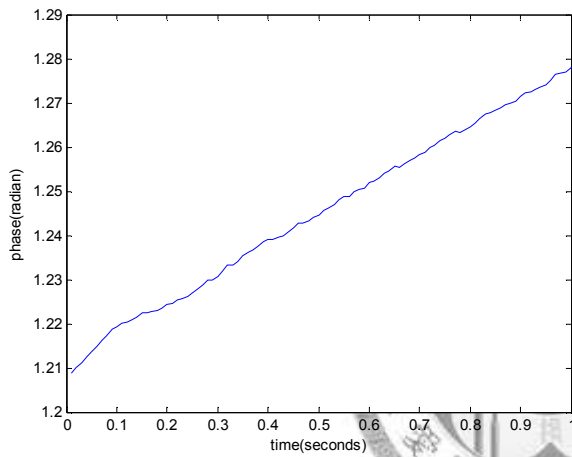
Fig.4-1 Geometry of the transmission experiment

The performance discussed in next section will separate into three parts:

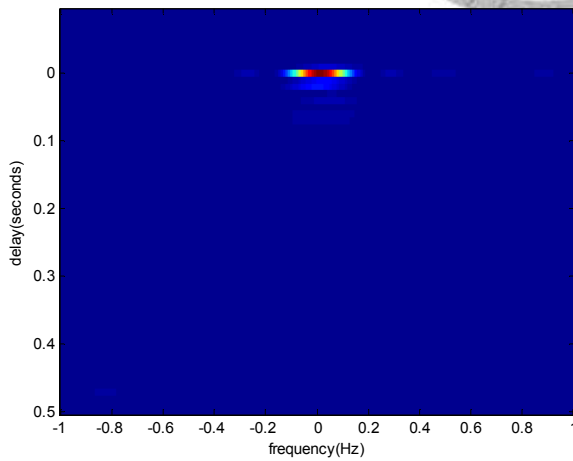
Case1: Receivers without the effect of internal wave, an example of channel condition is shown in figure 4-2, which is with low phase variation, channel fluctuation , and small Doppler spread bandwidth.



CIR variation



Phase variation (direct path)



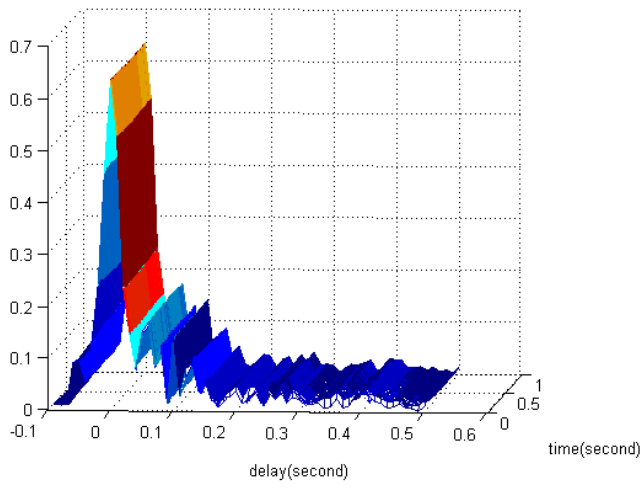
Scattering function

Fig.4-2 channel condition-ASIAEX day126-6:17:58 (channel 16)

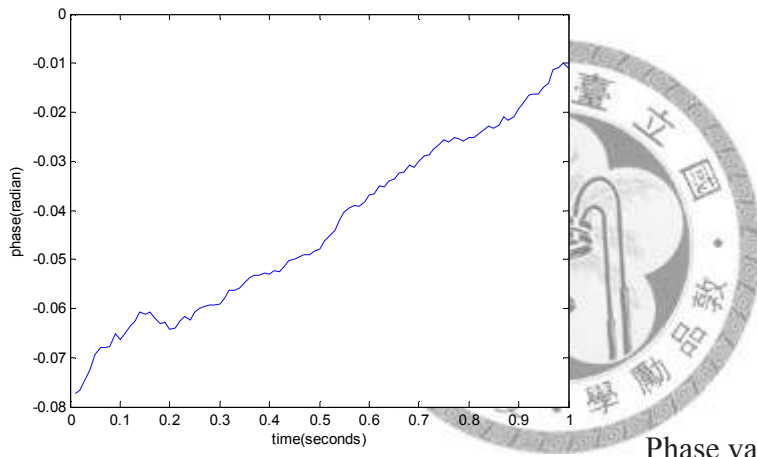
Case2: Internal wave approach the receivers, an example of channel condition is shown

in figure 4-3, and compare with case1 the channel become more severe fading,

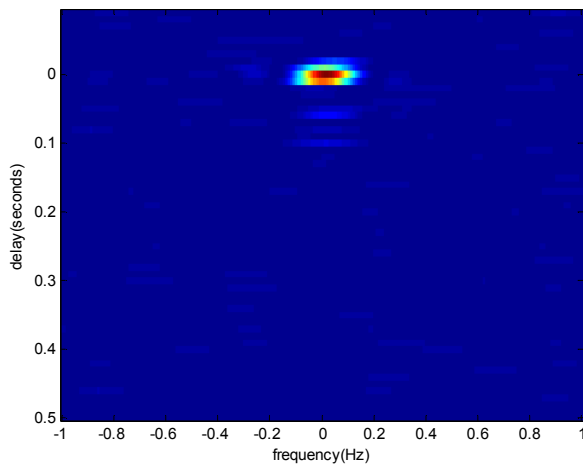
but it's not vary significant.



CIR variation



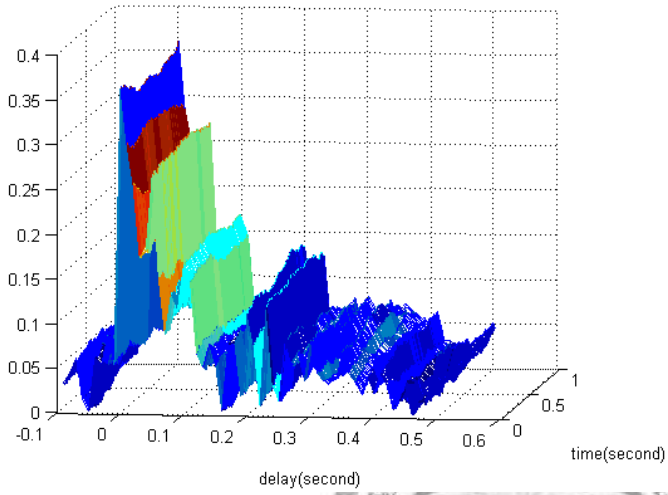
Phase variation(direct path)



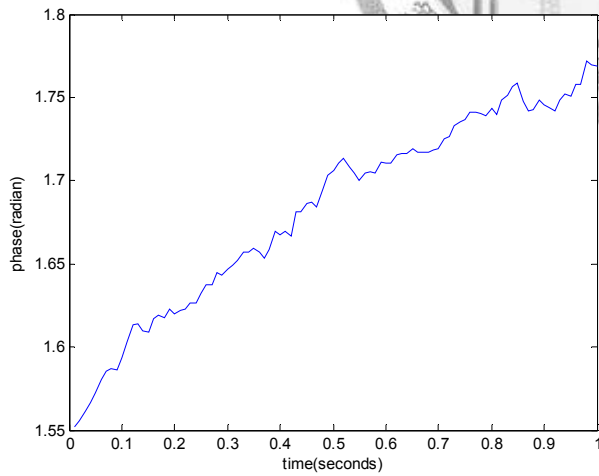
Scattering function

Fig.4-3 channel condition-ASIAEX day 128-9:46:3(channel 16)

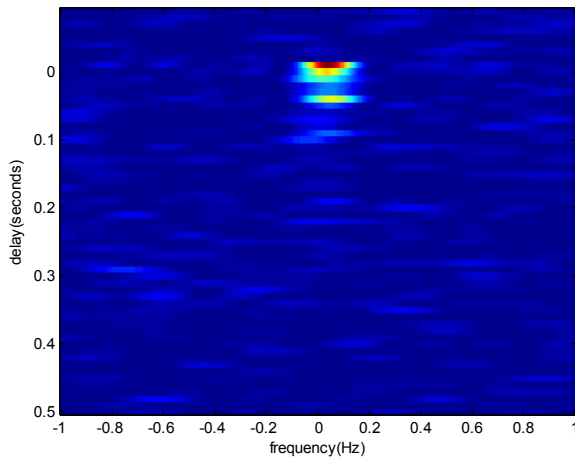
Case3: Internal wave reach the receivers, an example of channel condition is shown in figure 4-4, which is with high phase variation, channel fluctuation, and large Doppler spread than case 1 and case 2.



CIR fluctuation



Phase variation(direct path)



Scattering function

Fig.4-4 channel condition-ASIAEX day 128- 12:50:04(channel 16)

## 4.2 Signal-To-Multipath Ratio (SMR)

Underwater acoustic communications differ from RF communications in two major aspects. One is the long multipath delay time covering tens to hundreds of symbols and the other is temporal variation of the acoustic channel at a time scale on the order of communication packet length. The specifics are environment dependent. Consequently the performance is not uniform and its prediction capability has so far eluded the community. The channel impulse response function has been commonly used as an indicator for the channel effect on communications. In general, for phase coherent acoustic communications, the channel equalizer performance will degrade if there are many multipath arrivals that are unstable, i.e., fluctuating rapidly with time.

In the following, we will introduce a metrics, SMR, which can reflect the quality of channel.

The SMR introduced by Zielinski et al. [18] is a convenient measure for evaluating the communication link quality of the channel. Corresponding to the impulse response function of the channel, every delayed version of the transmitted symbol will corrupt the received signal. This is known as ISI. The corruption is proportional to the ratio of the delay to the symbol period. Two parameters are formed: the signal strength  $S$  and the multipath strength  $M$ . The estimation of  $S$  and  $M$  allows us to define a signal-to-corruptive multipath ratio, SMR, which is used in a similar manner to the signal-to-noise ratio in a noise-limited channel. In the formula form, the SMR of baseband signal is defined as:

$$SMR = \frac{|S|}{|M|} = \frac{|S_{dir}|}{\sum_{i=1}^{\infty} |S_i| - |S_{dir}|} \triangleq \frac{|h_{dir}|}{\sum_{i=1}^{\infty} |h_i| - |h_{dir}|}$$

Where  $|S_{dir}|$  denote the amplitude of direct path signal, and  $|h_{dir}|$  denote the amplitude of the tap of the direct path in channel impulse response, and an explanatory graph is shown in Fig.4-5

When the signal-to-multipath ratio (SMR)  $> 1$ , it can be used as a measure of system robustness against ambient noise and interfering signals. Note that even for  $SMR < 1$  the channel can still be used for transmission, but with a certain probability of error. This error performance can be improved by using suitable error correcting coding.

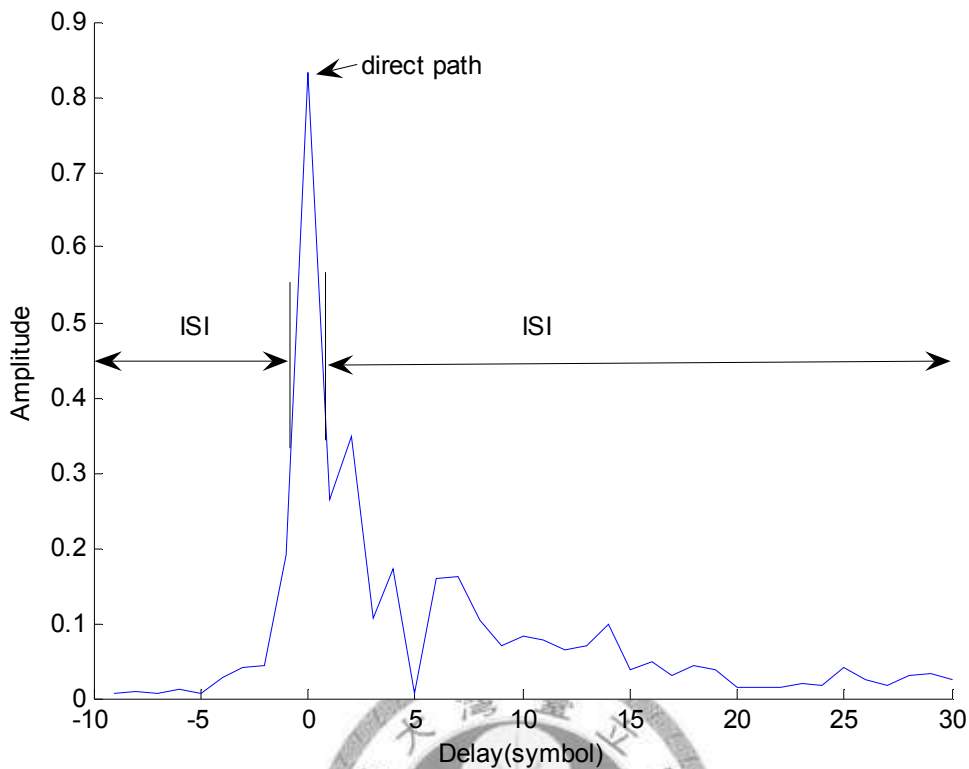


Figure 4-5 channel impulse response and the relation between direct path and multipath for ASIAEX –day 126-6:16:37 (channel 16), and the CIR correspond to  $SMR=1.7308$ .

And now we will compare the difference of SMR in different signal receiving time and different hydrophone receiving depth. Figure 4-6 shows the SMR measurement for different receiver depth, and it's obviously that the SMR monotonically increase with the receiving depth from channel 10 to channel 16, but for those channel near the surface , say, channel 1 to channel 10 , the SMR is relatively stable. Figure 4-7 shows some exactly impulse response of channels appeared in Figure 4-6. Low SMR sometimes indicate that signal has more chance to be interfered by delay spread or we can probably say that lower SMR relate to more severe signal



fading.

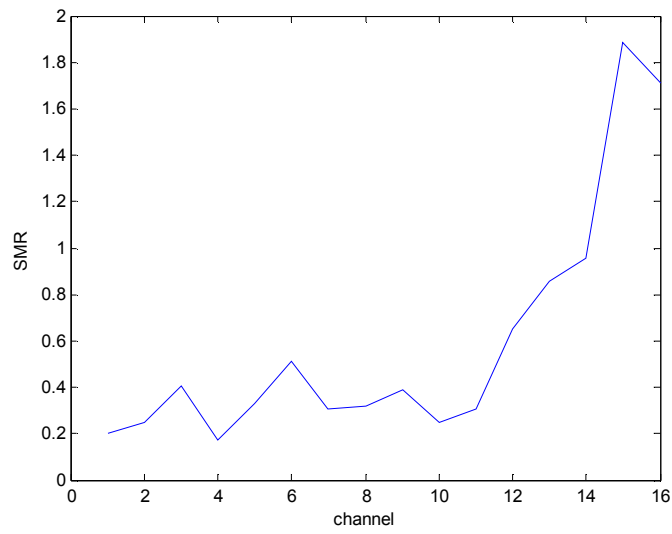
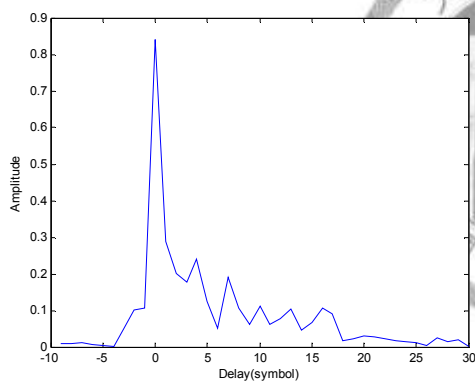
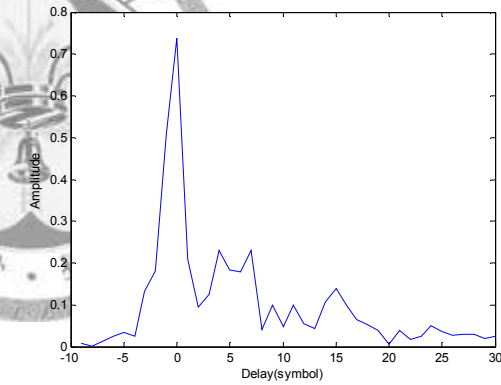


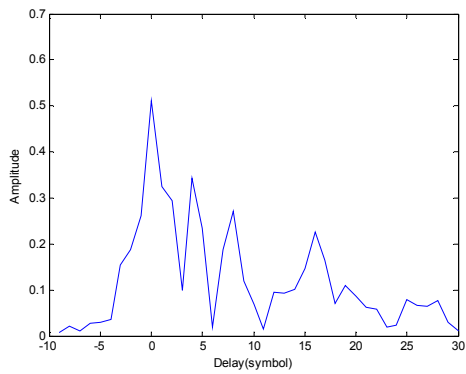
Figure 4-6 SMR of different channels (with different hydrophone depth) for ASIAEX-day126-6:15:42



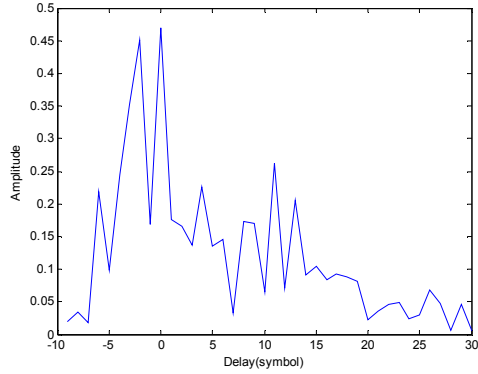
channel 15



channel 13



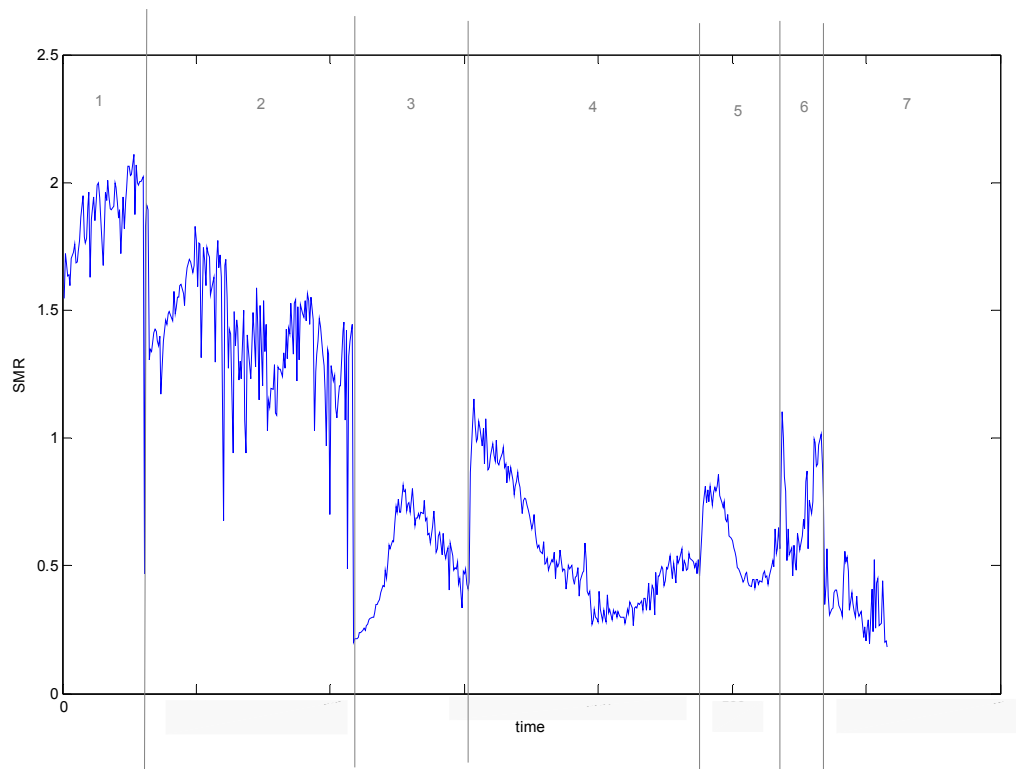
channel 8



channel 2

Figure 4-7 channel 15, 13, 8, 2 impulse response by pulse compression

Figure 4-8 and Figure 4-9 show the SMR of channels with different receiving time, it can be easily observed that even the receiver didn't suffer from the interference of internal-wave, for instance period of time 3 and 4, the signal must have the chance to confront severe ISI.



Time1: day 126-6:15:17 to 6:22:34 (the time of above sections aren't in the same scale)

Time2: day 127-4:15:28 to 4:52:41

Time3: day 127-5:15:36 to 6:19:56

Time4: day 127-6:45:19 to day 128-5:22:45 (rough trend of SMR in this period)

Time5: day 128-5:45:19 to 5:50:26

Time6: day 128- 9:45:33 to 11:46:12 (internal wave approach the receiver)

Time7: day 128-12:45:22 to 12:51:00 (internal wave reach the receivers)

Figure 4-8 SMR for different receiving time (channel 16)

Since we talked a lot about the SMR as an index for channel characteristic, we based on ASIAEX data showing that SMR is an index for fading condition. When  $SMR \ll 1$ , the fading is close to Rayleigh fading, which makes received signal severely attenuated together with large phase variation(close to uniform distribution). When  $SMR \gg 1$ , the fading is Rice fading and even closer to AWGN channel. Based on the ASIAEX data, we can see that when internal wave approaching, SMR become smaller and hence more severely faded.

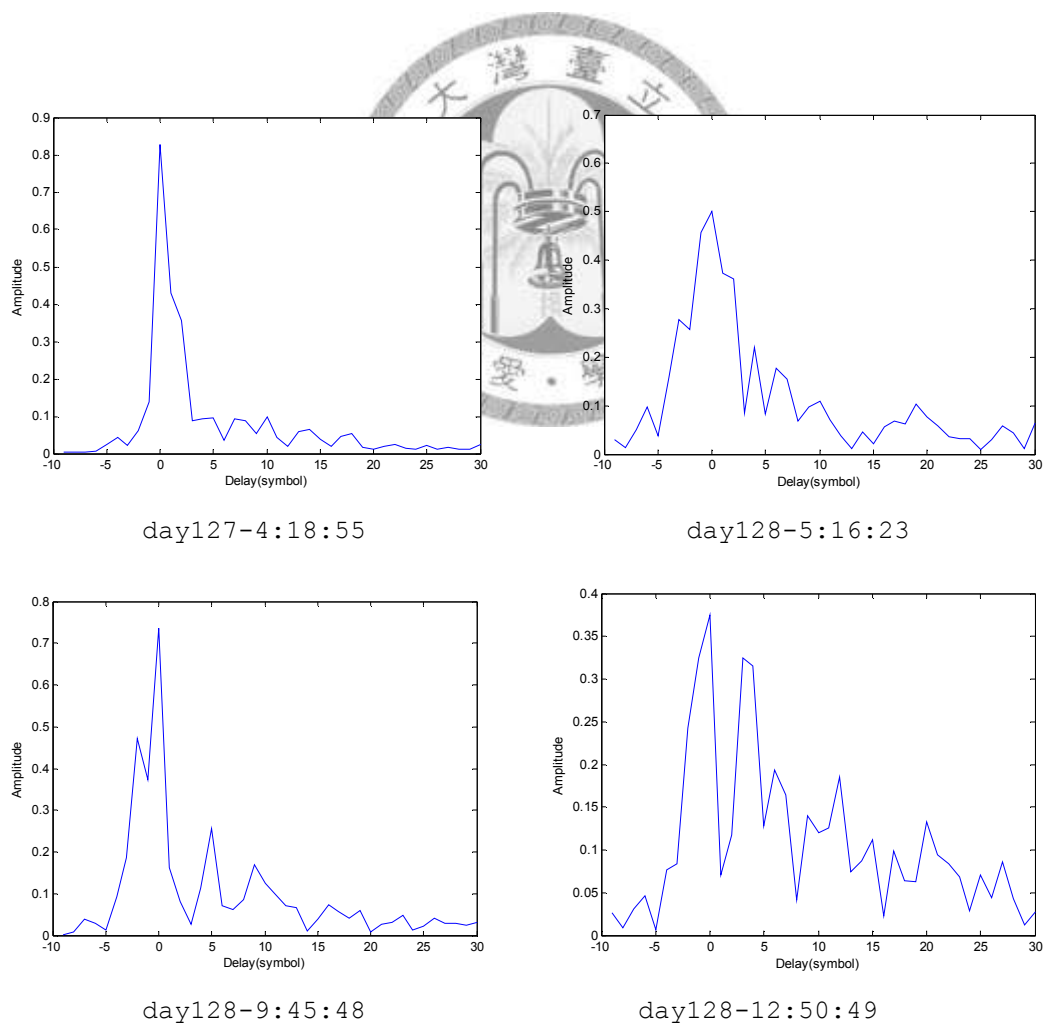
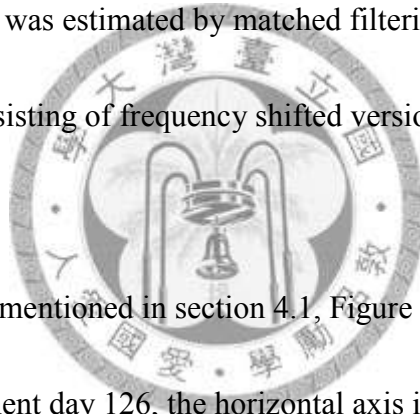


Figure 4-9 Instantaneous channel impulse response by pulse compression

### 4.3 Performance & Results

The acoustic signals received from each of the transmissions were processed to yield estimates of the time-varying channel impulse response, and scattering function of the acoustic channel. The received signals for the maximum length sequence (m-sequence) transmissions were demodulated, receiving filtered, and then sampled to baseband sequence. The channel impulse response was estimated by pulse compression as the real acoustic CIR, and tracked by RLS as the experiment acoustic CIR. The channel scattering function was estimated by matched filtering the received baseband signal with a sequence consisting of frequency shifted versions of the transmitted 511point m-seq.



Let's start from case1 mentioned in section 4.1, Figure 4-10 shows the value of SMR at 6:15:17 of experiment day 126, the horizontal axis is channel index from 1 to 16. We can observe that SMR increases when  $\lambda$  increases from channel 11 to channel 16, which are farther from surface than channel 1 to channel 10 are.

Figure 4-11 shows the snapshot of CIR of channel from 1 to 16, the CIR is estimated by pulse compression, and Figure 4-12 shows the scattering function of all channels, which can reflect the channel fluctuation.

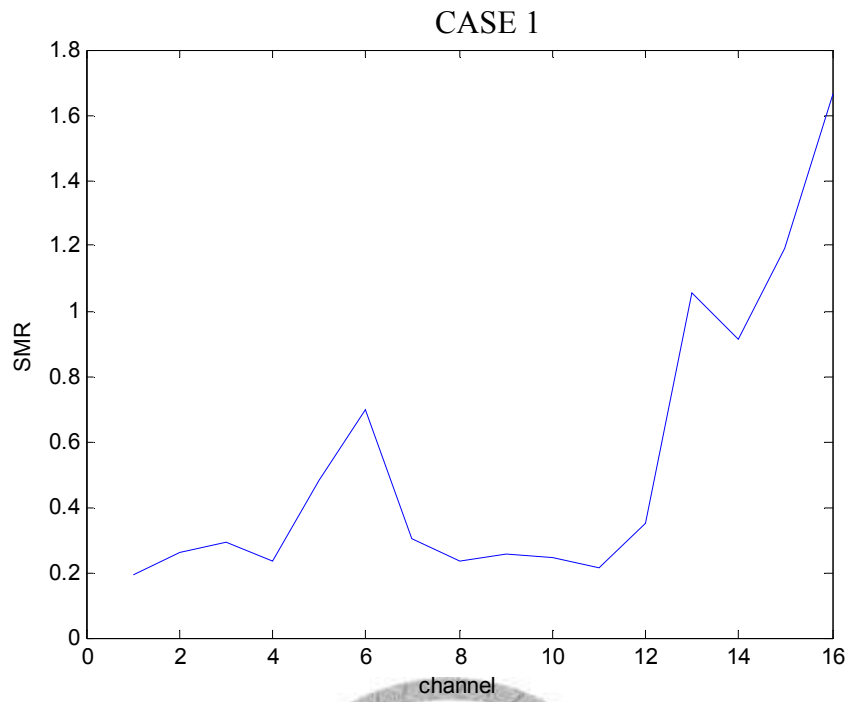


Fig. 4-10 SMR of channel 1~16 (day 126 - 6:15:17)

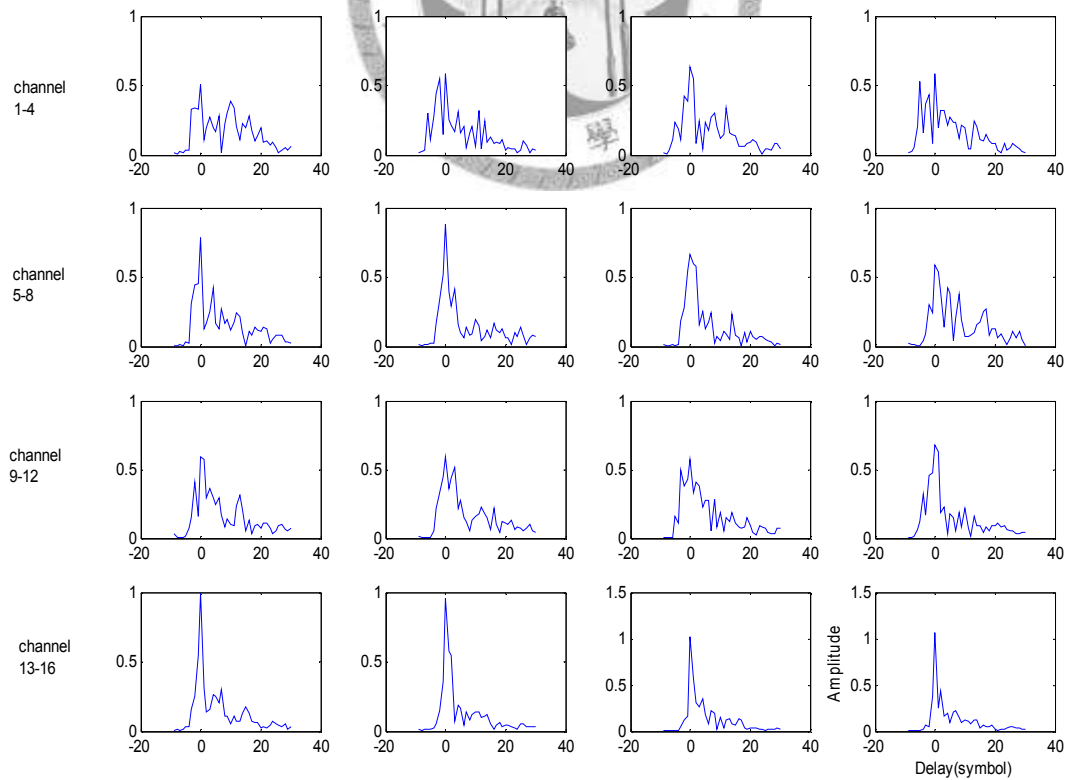


Fig. 4-11 CIR of channel 1~16 (day 126 - 6:15:17)

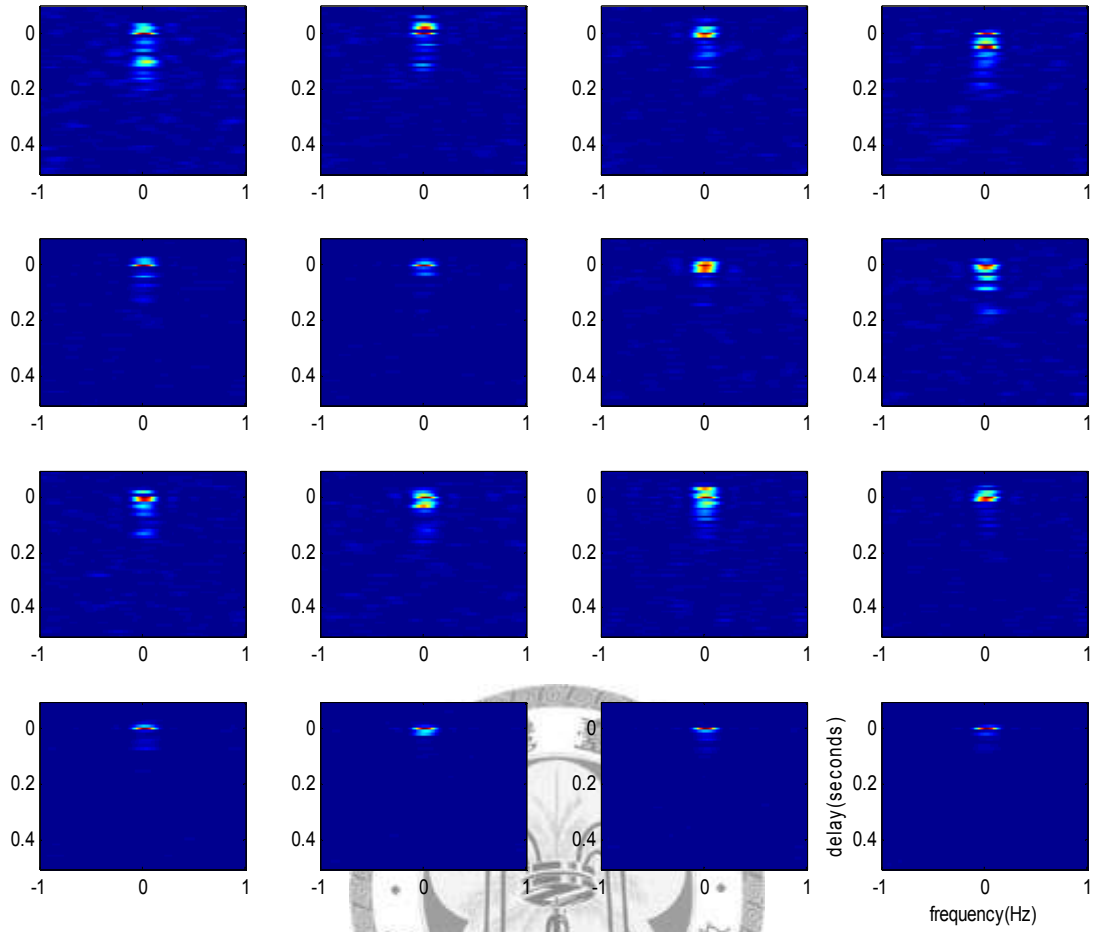


Fig. 4-12 scattering function of channel 1~16 (day 126 - 6:15:17)

Fig. 4-13, Fig. 4-14, and Fig. 4-15 show the performance of forgetting factor prediction, compared together with the experiment value, and the prediction value. The experiment value can be obtained by multi-parameter trial, expressed as:

$$\lambda_{\text{opt}} = \arg \min_{\lambda} \lim_{k \rightarrow \infty} E(\|\mathbf{h}_k - \hat{\mathbf{h}}_{k,\lambda}\|^2)$$

$\mathbf{h}_k$  is calculated by pulse compression,  $\hat{\mathbf{h}}_k$  is obtained by RLS.

And the result like the Figure 3-1 shows, it has a minimum value.

The prediction value can be obtained by the proposed method discussed in section

3. The statistic,  $M$ , discussed in section 3.1, first set to 10 to predict the optimal

forgetting factor, and the result is shown in Fig. 4-13. It's obvious that the prediction value is very close to the experiment value at channel 10 to channel 16. It seems that when the channel is relatively stable for the receivers far away from the surface, the prediction needn't too much statistic.

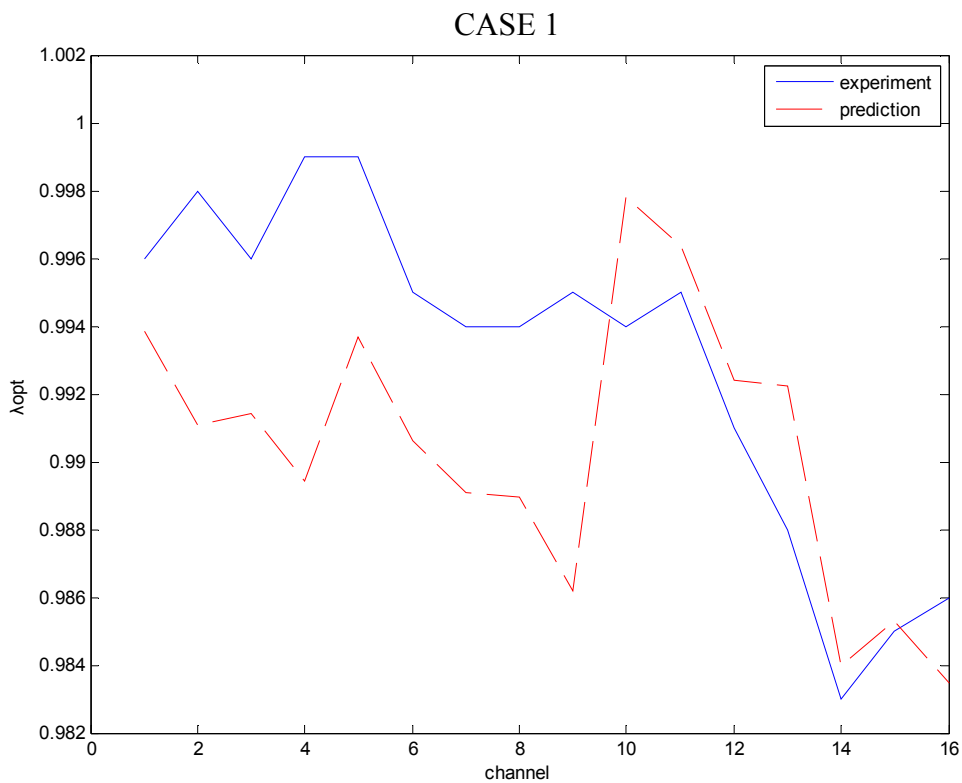


Fig. 4-13 performance of optimal forgetting factor prediction(M=10)  
(day 126 - 6:15:17)

Fig. 4-14 shows the performance result of M=20, and we can observe that the prediction accuracy of channel 1 to channel 9 increase when the statistic increase to 20. It can be explained that the severe fading channel need more statistic to capture the channel characteristic.

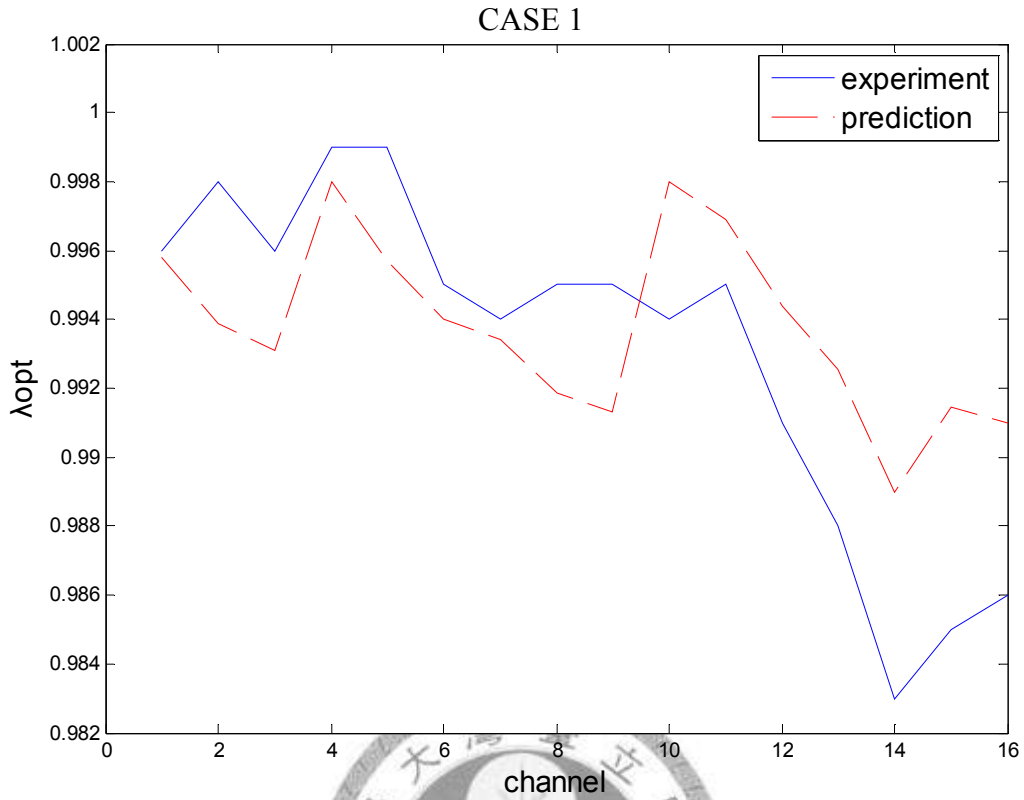


Fig. 4-14 performance of optimal forgetting factor prediction (M=20)  
(day 126 - 6:15:17)

Fig. 4-15 shows the performance result of M=30, and we can observe that the improvement of prediction accuracy is not very significant, and for some channels, for instance channel 14, the accuracy is growing worse. So in the following performance comparison, the statistic, M, is set to 20.

Fig. 4-16 shows the channel estimation mean square error for 100 iterations, and can be expressed as:

$$\xi = E(\|\mathbf{h}_k - \hat{\mathbf{h}}_{k,\lambda}\|^2)$$

It shows that the channel estimation MSE of the prediction forgetting factor very



approach the minimum channel estimation MSE.

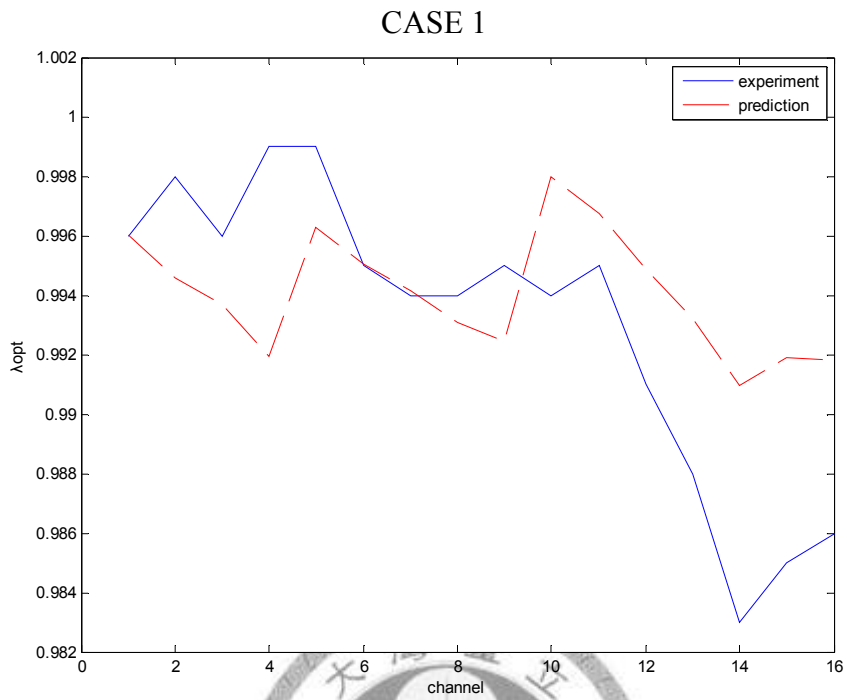


Fig. 4-15 performance of optimal forgetting factor prediction(M=30)  
(day 126 - 6:15:17)

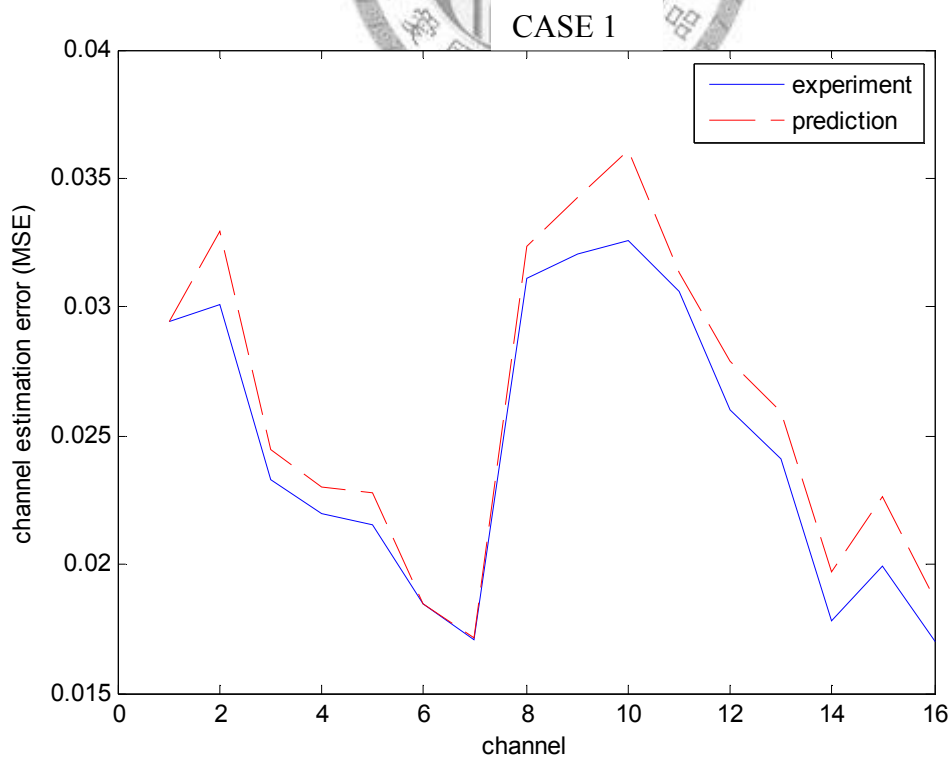


Fig. 4-16 channel estimation error (day 126 - 6:15:17)

Here is another experiment result, which is for case 2, experiment day 128 at 9:46:53

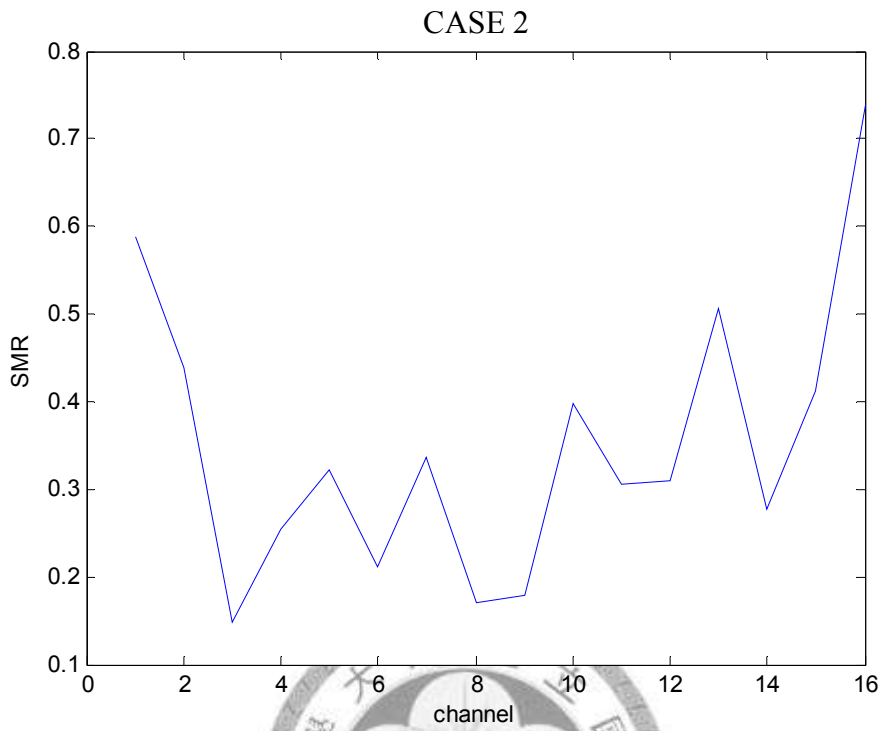


Fig. 4-17 SMR of channel 1~16 (day 128-9:46:53)

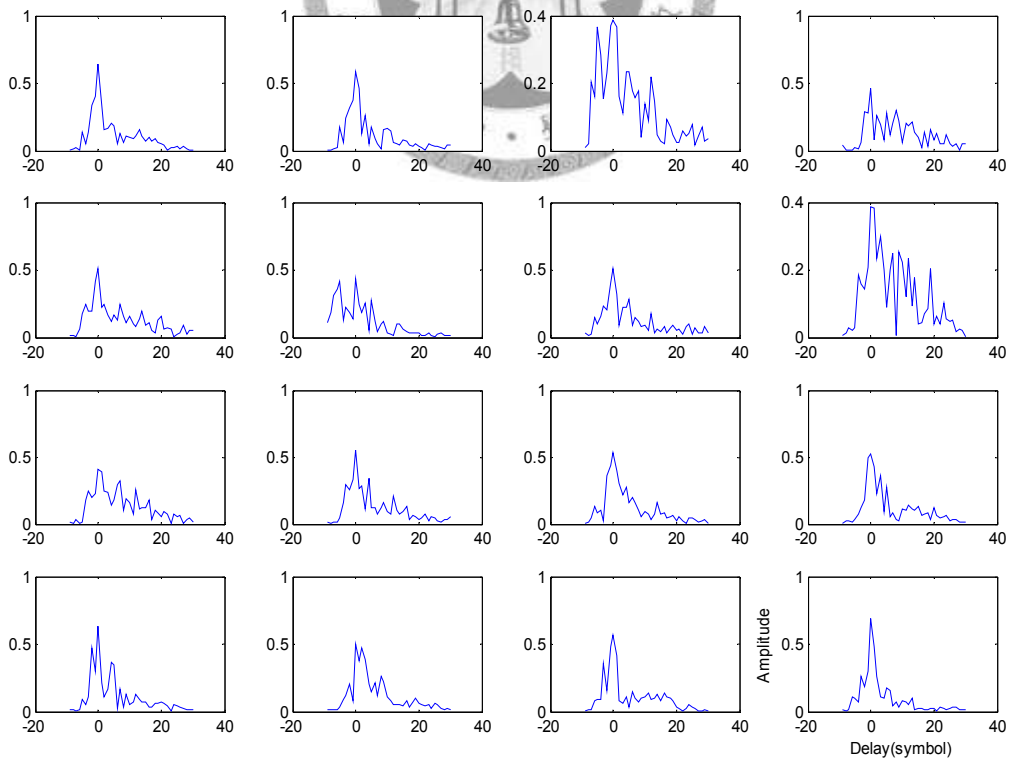


Fig. 4-18 CIR of channel 1~16 (day 128-9:46:53)

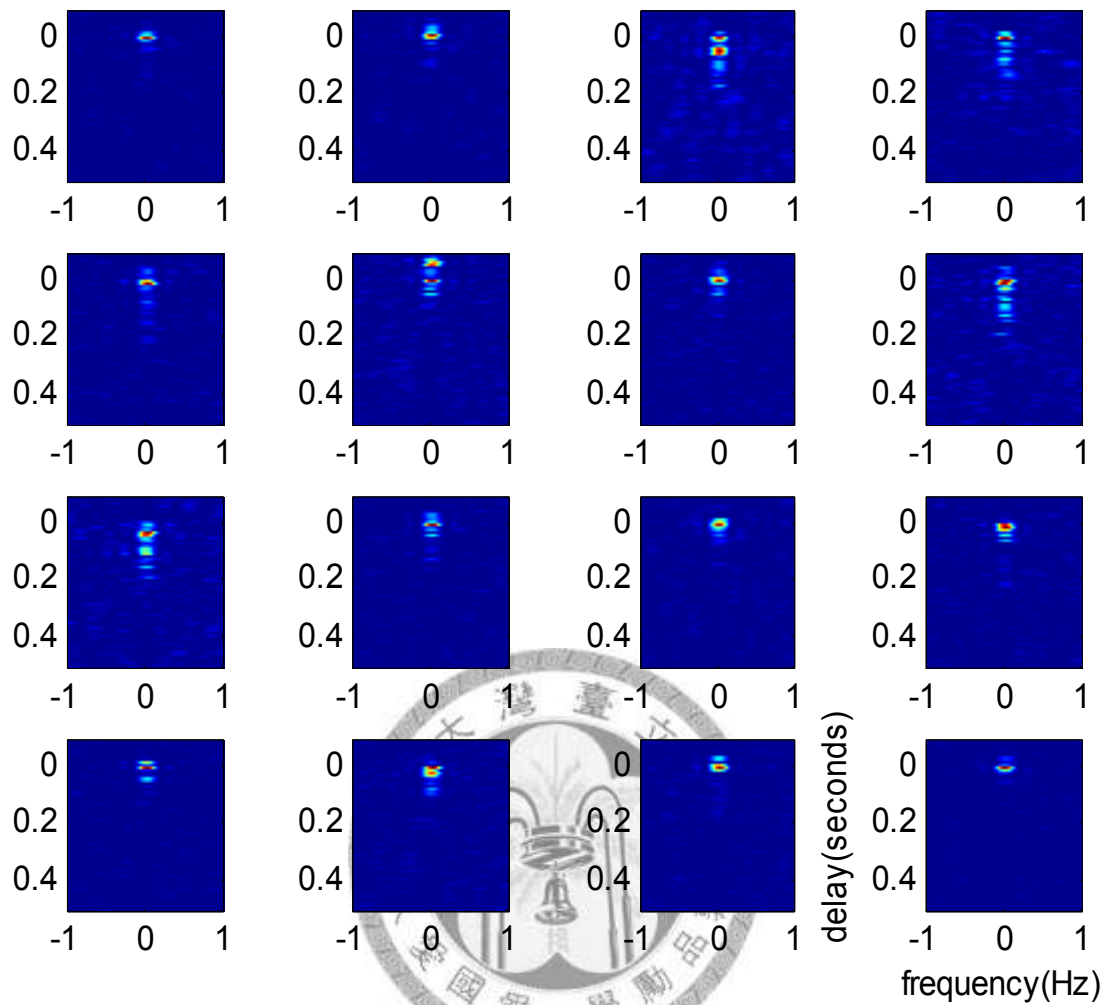


Fig. 4-19 scattering function of channel 1~16 (day 128-9:46:53)

Observe the scattering function of channel 3, 4, and 9 in Fig. 4-19, and compare with the performance of optimal forgetting factor prediction of these three channels in Fig. 4-20. It was evident that the prediction accuracy is greatly related to the channel fluctuation. The cause of this fluctuation must be internal wave or undulation of the surface. And Comparing Figure 4-16 and Figure 4-21, channel estimation error is growing up for some channels, this phenomena can be impute to the internal wave interfere with the receivers.

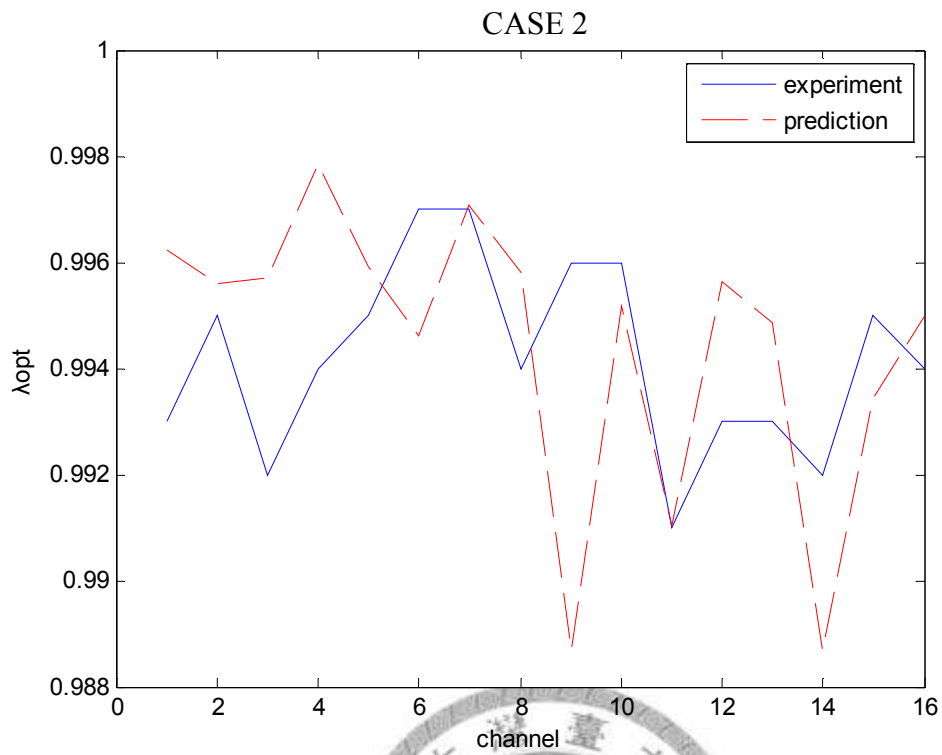


Fig. 4-20 performance of optimal forgetting factor prediction (M=20)

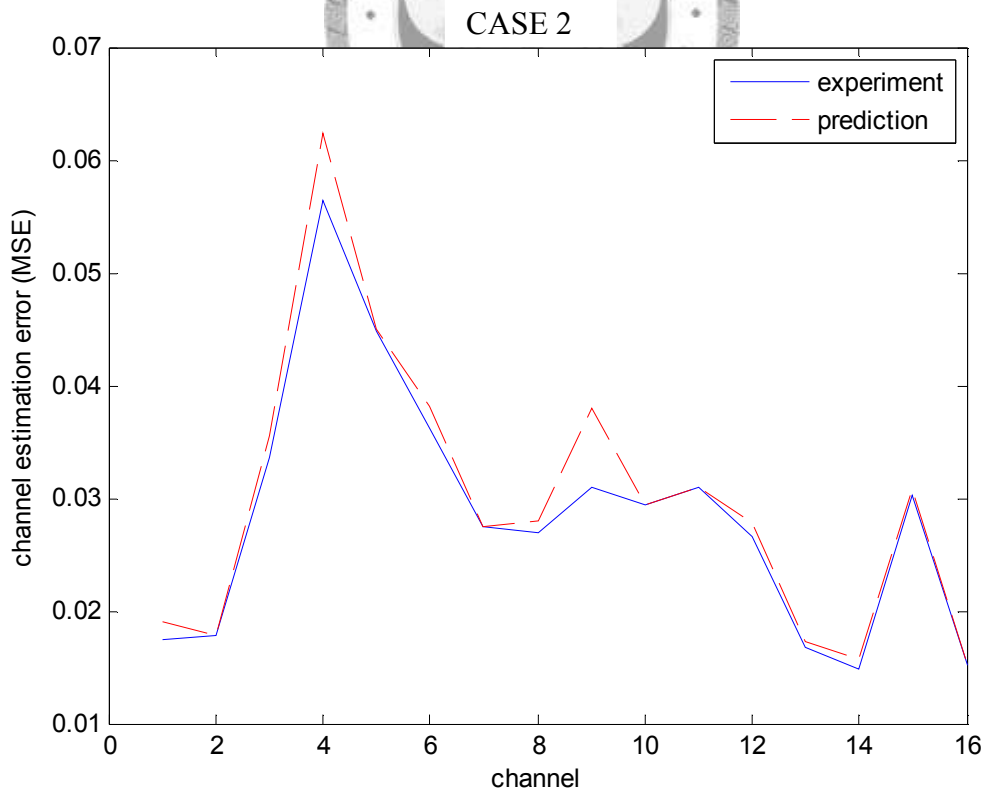


Fig. 4-21 channel estimation error (day 128-9:46:53)

And the experiment result of last case shown in Fig. 4-22 to Fig. 4-26, it's for case 3, and the experiment day is day-128 at 12:46:03.

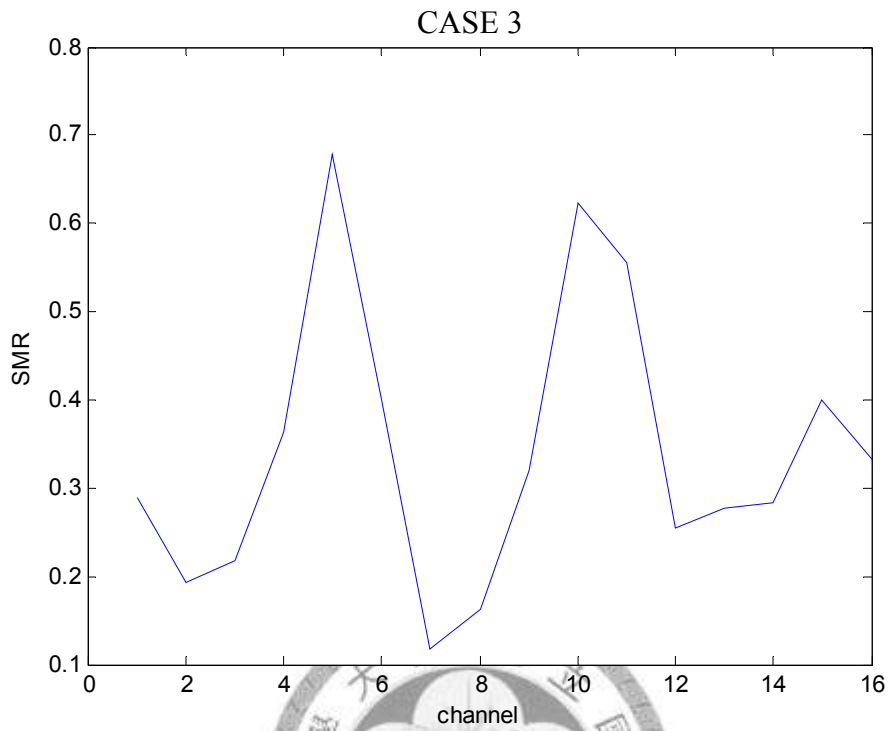


Fig. 4-22 SMR of channel 1~16 (day 128-12:46:03)

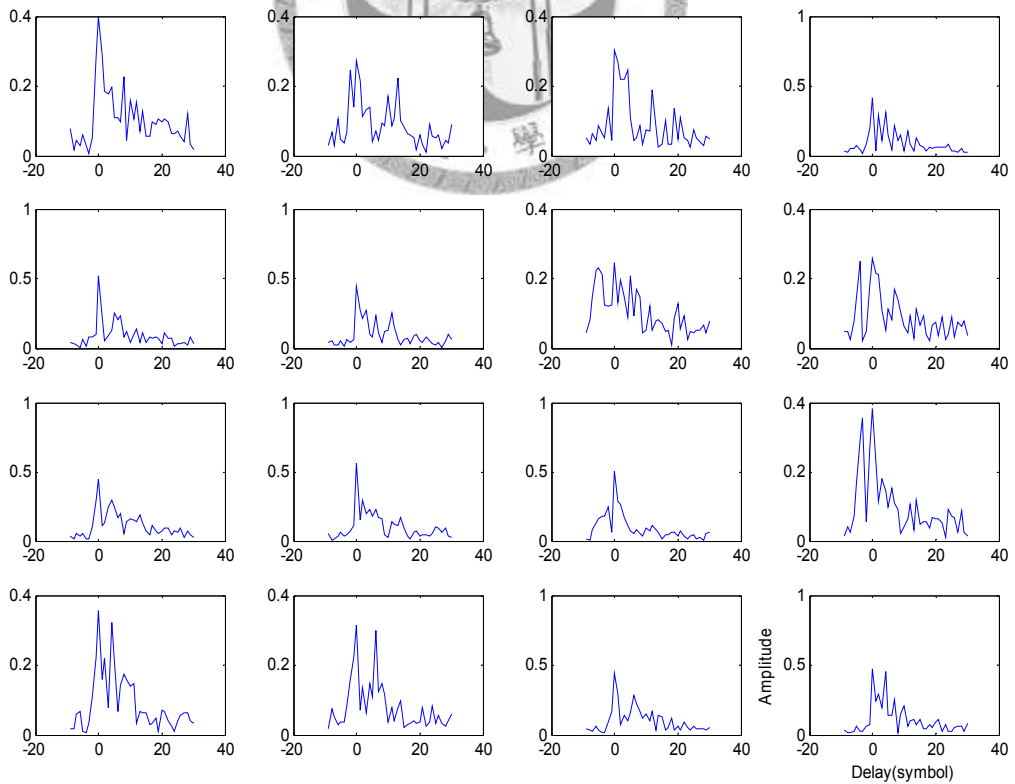


Fig. 4-23 CIR of channel 1~16 (day 128-12:46:03)

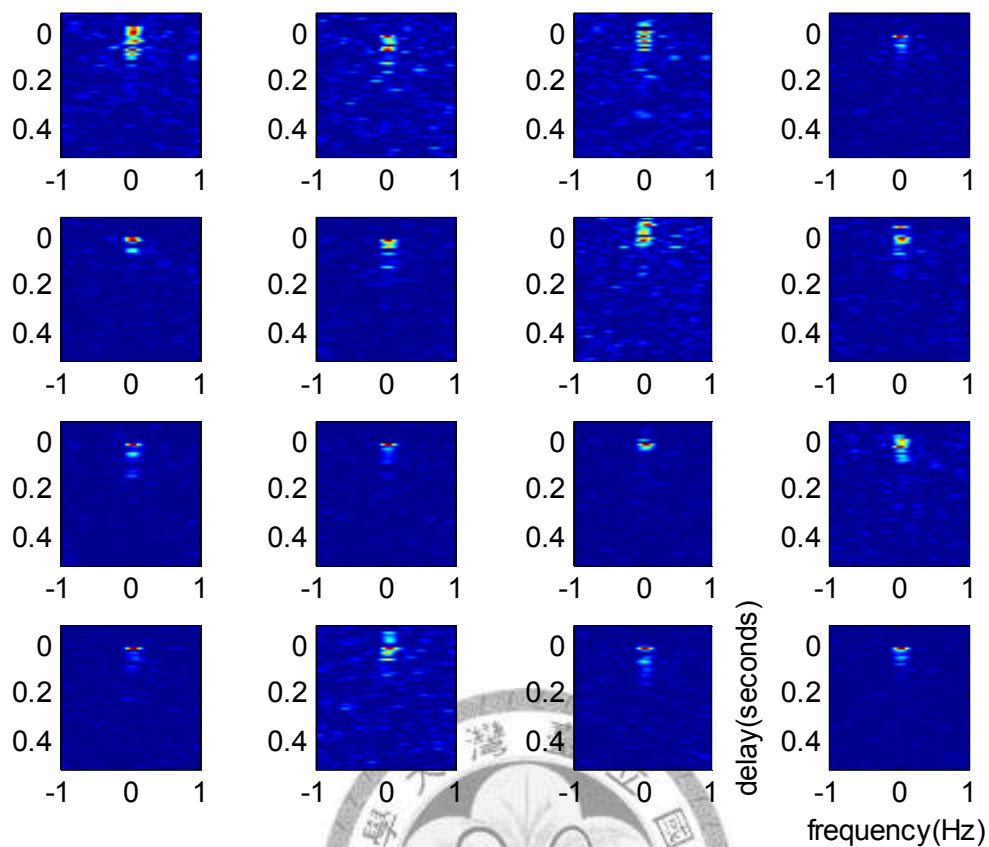


Fig. 4-24 scattering function of channel 1~16 (day 128-12:46:03)

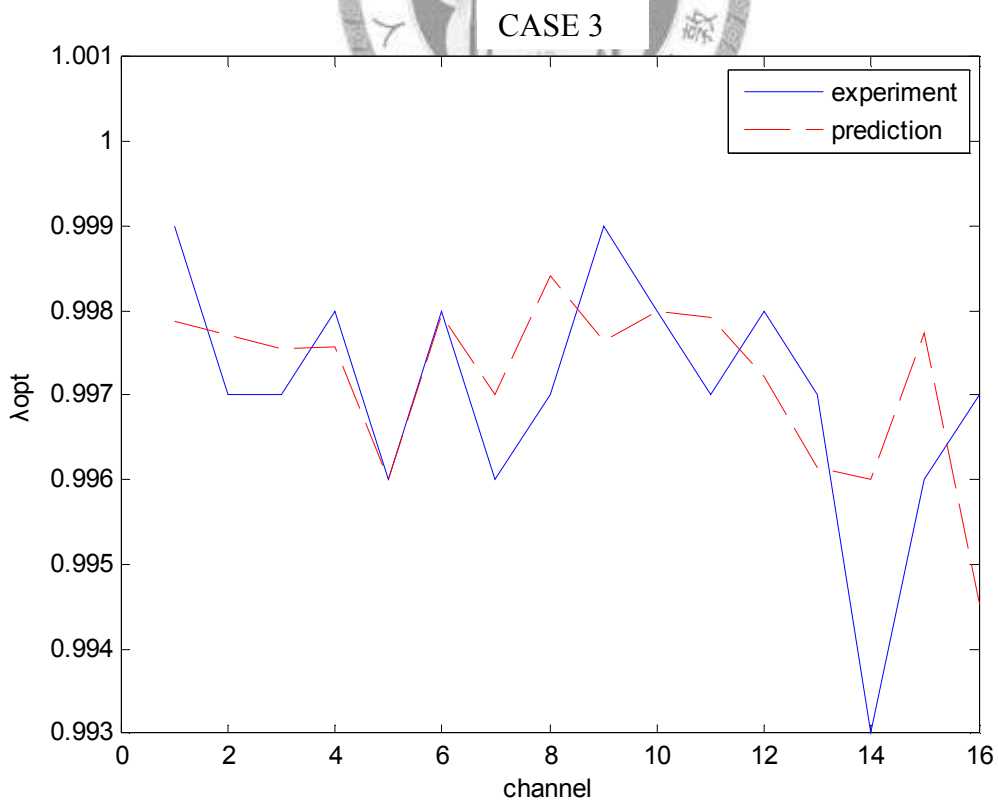


Fig. 4-25 performance of optimal forgetting factor prediction (M=20)

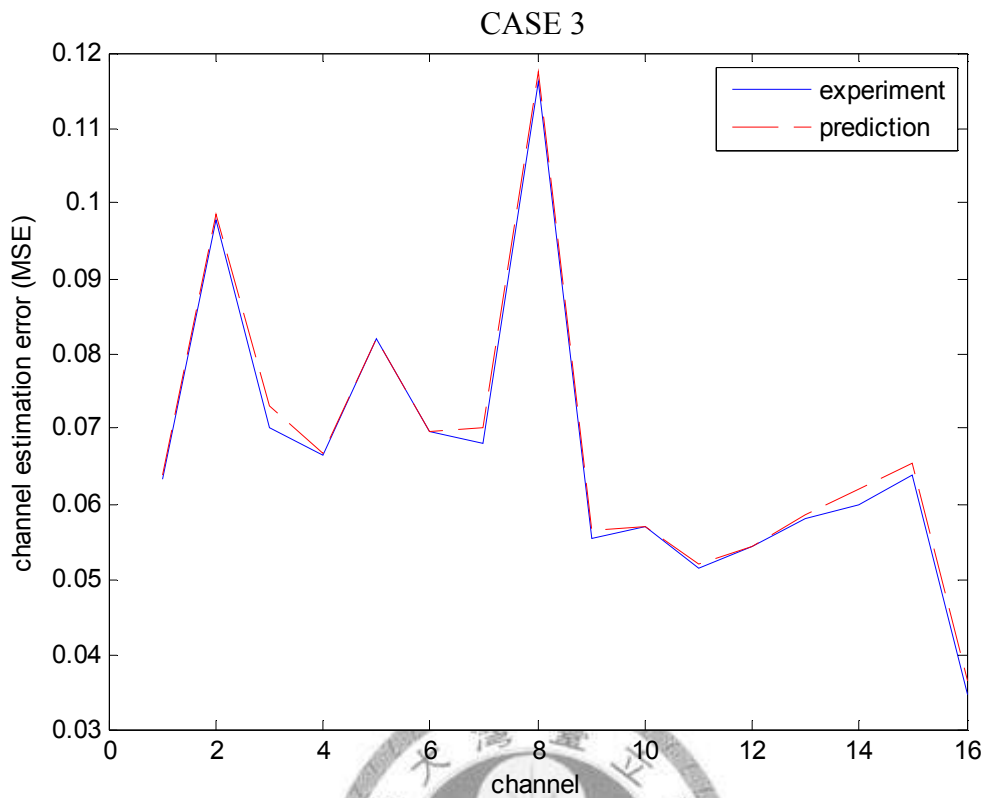


Fig. 4-26 channel estimation error (day 128-12:46:03)

Observe the estimation result of forgetting value in the severe time-varying channel, say, near the surface or suffered from interval-wave. The comparison is shown in Fig.4-27. It shows that the value is more larger than the value of calm channel.

Since we talk about more severe fading, much lower value of forgetting factor, but the result is negative, now consider with the channel dimension. The effective averaging window length of the RLS algorithms is  $1/(1-\lambda)$ . In general, the averaging window length should be proportional to the channel dimension (a rule of thumb value is 2–3 times the channel length) to maintain the stability of the algorithms [19].

So, it seems the optimal forgetting factor value depends on two factors:

1) Fading rate: Faster time varying channel imply smaller  $\lambda$  value.

2) Channel dimension: Larger dimension imply large  $\lambda$  value.

Compare these three cases as shown in Fig.4-27 and Fig.4-28, it seems that the channels near the surface are similar to the internal wave channels, smaller forgetting factor, lower SMR, faster channel fluctuation, and larger Doppler spread etc. But the channel estimation error is very huge in case 3, even with the optimal forgetting factor. It indicates that the RLS algorithms can't fully follow with the fluctuation of internal wave channel.

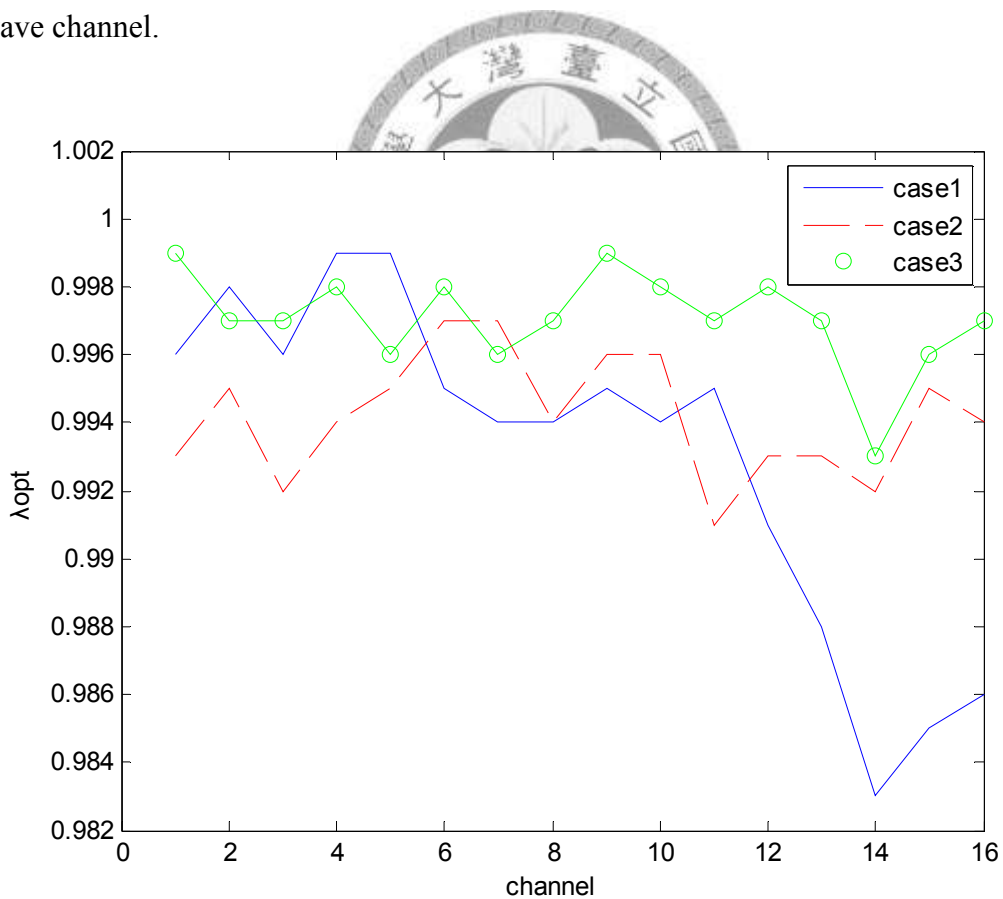


Fig.4-27 optimal forgetting factor comparison of these three cases



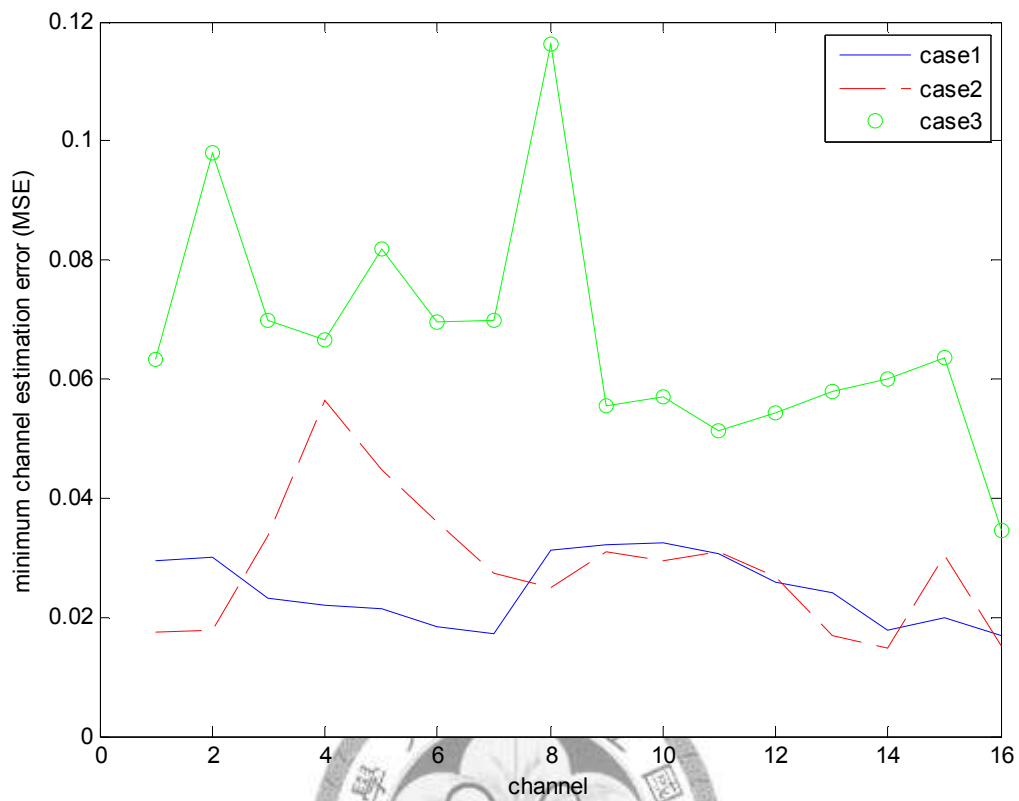
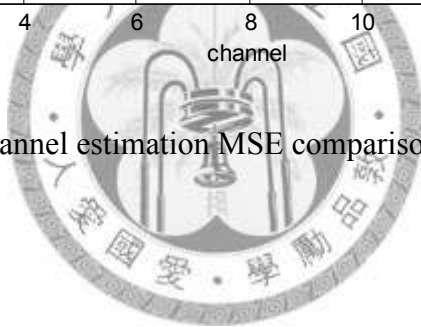


Fig.4-28 minimum channel estimation MSE comparison of these three cases



## Chapter5 Conclusion

1. In the experiment result, we can observe that the proposed Forgetting Factor estimation is effective, even for severe fading channel, which is near the surface or with internal-wave interference.
2. It's obvious that the value of optimal Forgetting Factor is highly correlated to the channel fading rate and SMR.
3. Faster time varying channel imply smaller FF value, and lower SMR means lager delay-spread, it may bound the FF value in order to maintain the stability of the algorithms, but the tracking capacity was degraded, this phenomenon can be observe in those channels near the surface, or with the internal wave interference.
4. The proposed approximate optimal forgetting factor estimation confirms that the channel estimator maintain the minimum channel estimation MSE by using the estimated FF value in the data receiving period.

## Reference

- [1] M. Chitre ,S. S. Shahabudeen ,M. Stojanovic,” Underwater Acoustic Communications and Networking: Recent Advances and Future Challenges ”, MTSJ 2008
- [2] D. B. Kilfoyle, A. B. Baggeroer, ”The state of the art in Underwater Acoustic Telemetry”, IEEE J. OCEANIC ENG., VOL. 25, NO. 1, JANUARY 2000
- [3] G. M. Wenz, Acoustic ambient noise in the ocean: spectra and sources, J. Acoust. Soc. Am. 34, 1936-1956 (1962).
- [4] S. Haykin, Adaptive Filter Theory, Third ed. Englewood Cliffs, NJ:Prentice-Hall, 1996.
- [5] B. Toplis and S. Pasupathy, “Tracking improvements in fast RLS algorithms using a variable forgetting factor,” IEEE Trans. Acoust., Speech, Signal Process., vol. 36, no. 2, pp. 206–227, Feb. 1988.
- [6] T. R. Fortescue, L. S. Kershenbaum, and B. E. Ydstie, “Implementation of self-tuning regulators with variable forgetting factors,” Automatica, vol. 17, pp. 831–835, 1981
- [7] D. J. Park et al., “Fast tracking RLS algorithm using novel variable forgetting factor with unity zone,” Electron. Lett., vol. 27, pp. 2150–2151, Nov. 1991.
- [8] S. Song et al., “Gauss Newton variable forgetting factor recursive least squares for time varying parameter tracking,” Electron. Lett., vol. 36, pp. 988–990, May 2000.
- [9] S.H. Leung and C. F. So, “Gradient-Based Variable Forgetting Factor RLS Algorithm in Time-Varying Environments”, IEEE Trans.Signal processing, vol. 53, no. 8, August 2005
- [10] D. R. Dowling, “Acoustic pulse compression using passive phase conjugate processing,” J. Acoust. Soc. Amer., vol. 95, no. 3, pp. 1450-1458, 1994.
- [11] J. G. Proakis, Digital Communications, 3rd ed. \_McGraw-Hill, New York, 1995\_, Chaps. 13 and 14, pp. 724–729.
- [12] H. L. Van Trees, Detection, Estimation, and Modulation Theory, Part III \_Wiley Inter-Science, New York, 2001\_, Chap. 13.
- [13] J. C. Preisig, Performance analysis of adaptive equalization for coherent acoustic communications in the time-varying ocean environment. J. Acoust. Soc. Am., 118(1):263–278, July 2005.
- [14] M. Stojanovic, J.G.Proakis and J.A.Catipovic, “Performance of High-Rate Adaptive Equalization on a Shallow Water Acoustic Channel”, 127th Meeting of the Acoust. Soc. Am., Cambridge, MA, 95, 2809-2810 (1994).
- [15] O. Macchi, Adaptive processing: The LMS Approach with applications in

- Transmission, Wiley, New York, 1995
- [16] E. Eweda, "Comparison of RLS, LMS, and sign algorithms for tracking randomly time-varying channels," *IEEE Trans. Signal Process.*, vol.42, pp.2937–2944, Nov. 1994.
- [17] S. R. Ramp, J. F. Lynch, P. H. Dahl, C.-S. Chiu, and J. A. Simmen, "ASIAEX fosters advances in shallow-water acoustics," *EOS, Trans. AGU*, vol. 84, no. 37, pp. 361– 367, 2003.
- [18] A. Zielinski, Y. Yoon, and L. Wu, "Performance analysis of digital acoustic communication in a shallow water channel," *IEEE J. Oceanic Eng.*, vol. 20, pp. 293–299, Oct. 1995.
- [19] W. Li, J. Preisig "Estimation of Rapidly Time-Varying Sparse Channels" in *IEEE Journal of Oceanic Engineering*, 2006.

